DEVELOPMENT AND APPLICATION OF AN INTERFEROMETRIC SYSTEM FOR MEASURING CRACK DISPLACEMENTS

Final Report on Grant NSG 1148

March 1, 1975 -- June 30, 1976

W. N. Sharpe, Jr.

Division of Engineering Research
Michigan State University
East Lansing, Michigan 48824

DEVELOPMENT AND APPLICATION OF AN INTERFEROMETRIC SYSTEM FOR MEASURING CRACK DISPLACEMENTS

Final Report on Grant NSG 1148
March 1, 1975 -- June 30, 1976

W. N. Sharpe, Jr.

Division of Engineering Research
Michigan State University
East Lansing, Michigan 48824

ABSTRACT

The interferometric displacement gage (IDG) is a laser-based technique that measures the relative displacement of reflecting indentations in a metal surface. Movement of the two interference fringe patterns emanating from the closely spaced indentations is related to the in-plane displacement. This report presents the development of the first version of a minicomputer controlled system that converts the fringe pattern motion into a voltage output proportional to displacement. Details of the instrument and the calibration tests are included.

The small displacement technique has a resolution of 0.004 microns and a range of 0.14 microns in this first version. The range can be extended with further software development. The large-displacement technique has a resolution of 0.25 micron and a range of 400 microns. Its range depends on the size of the laser beam and can be as large as 3 mm. The error bands based on the calibration experiments are 5 percent and 1 percent, respectively, for the small and large displacement techniques. These specifications are based on calibration experiments with this first prototype. Software to average fringe shifts, account for direction of fringe motion, etc., would greatly improve the capabilities of the instrument.

The gage length of the IDG can be as small as 50 microns. As such, it has potential for measuring displacements near the tips of fatigue cracks. Measurements on a fatigue-cracked specimen are included to demonstrate this.

An Addendum is attached describing further software development after the grant's expiration. The new software accounts for fringe direction and permits the large-displacement technique to be used for cyclic loading with a resolution of 0.12 microns.

ACKNOWLEDGEMENTS

The author wishes to acknowledge the support and guidance of the Technical Officer, Dr. Wolf Elber. The very capable assistance of Mr. Gary Bergeron, who assembled the electronics and developed the first software version, is recognized as a major contribution. Mr. Dennis Anderson's development of a second software program is also greatly appreciated.

TABLE OF CONTENTS

1. INTRODUCTION

Fracture mechanics is based on the behavior of material in the neighborhood of a crack tip. The elastic stress analysis of this behavior is (in its simplest form) restricted to a region within a distance of approximately a/20 from the crack tip (where "a" is the crack length). Current nondestructive evaluation procedures that operate on a production basis for such critical elements as aircraft components can discover cracks on the order of 0.050 inches (1.25 mm) long. The localized region of the crack tip is then only on the order of 20 microns in length. A transducer that will measure displacement (or strain) in very small regions is governed by this size requirement. In practical laboratory testing of metal specimens, the cracks are larger--on the order of 0.5 inch (12.5 mm)--but the required transducer size is still smaller than conventional techniques allow.

One example of the usefulness of displacement measurements near fatigue crack tips is in the study of the closure phenomenon. Closure refers to the fact that cracks grown by fatigue loading do not open all the way along their length until a certain opening load is applied. This opening load may be 20 to 50 percent of the maximum load applied during crack growth. Obviously this is an important consideration because it means that at loads less than the opening load the "crack" is actually not as long as expected. The opening load can be established by measuring the displacement near the crack tip as load is applied; when the crack is fully open, load is linearly related to displacement. Elber [1, 2] developed a clip gage with an 0.05 inch (1.27 mm) gage length for closure measurements. Direct displacement measurements by photomicrography were made by Adams [3] using a gage length of 76 microns, but that is a very time-consuming technique. A simpler technique is to bond one end of a common foil resistance strain gage on each side of the crack and thus monitor the displacement [4]. Closure measurements based on the bulk response of a specimen have been made by Buck et al. [5] using ultrasonics and by Wei [6] using electrical resistance changes.

Another area where measurements near the crack tip are useful is in the determination of the stress intensity factor. Most of the experimental determination has been obtained by two- and three-dimensional photoelasticity, and those works are summarized in a comprehensive review paper by Smith [7]. Dudderar and Gorman [8] measured displacements

and thus the stress intensity factor in thin PMMA sheets using holographic interferometers. Sommer [9] and Crosby et al. [10] measured the displacements near a crack tip inside glass specimens using interferometry and then computed the stress intensity factor. All of these techniques require transparent models.

Surface displacements and strains on metal specimens can be measured with the moiré technique; see the review article [11]. This requires that high density grilles be printed on the polished specimen surface, and the data reduction can be laborious. Displacements perpendicular to the surface of opaque specimens can be measured with conventional interferometry, as discussed in another review article [12].

A different way of measuring in-plane surface displacement on metal specimens is a laser interferometry method referred to as the interferometric displacement gage (IDG). In this technique, the distance between two very small reflecting surfaces is measured interferometrically. The primary advantage of the IDG is that its gage length can be very small--as small as 50 microns. This means that displacement measurements can be made much nearer the crack tip than with other techniques. The IDG has been used for both closure measurements [13, 14] and stress intensity factor measurements [15]. In the closure measurements the interference fringes were photographed, and crack displacement was determined by comparing before-and-after load patterns. In the stress intensity factor measurements the fringe motion was recorded on a strip-chart recorder using photoresistors. Both of these data requisition and reduction schemes are very inefficient. The objective of this research was to automate the measurement using minicomputer control to produce a real-time voltage output proportional to displacement.

This report describes the initial development of a data acquisition and reduction process for the IDG. The first prototype of a working computerized system is described. This system can be greatly improved by future software developments; the hardware assembled appears adequate. The optical aspects of the IDG are first briefly reviewed in section 2. If one is to computerize an interference fringe measurement, one must first develop a way to transform the fringe position into a suitable electrical signal. The minicomputer system and fringe scanning system required for this are described in sections 3. The computer-controlled instrument

is developed for two magnitudes of displacement--high sensitivity with small range (less than 1 micron) and low sensitivity with large range (approximately 500 microns). These two different systems are described in sections 4 and 5. The large displacement scheme is applied to a couple of typical measurements in sections 6 and 7. Throughout the report suggestions are included as to software developments that can vastly improve the measurement capabilities of the instrument. Some potential applications are suggested and concluding remarks are given in section 8.

2. THE INTERFEROMETRIC DISPLACEMENT GAGE

The principle of this displacement gage can be understood with the aid of Figure 2.1. Shallow reflecting indentations are made on the two surfaces whose relative displacement is to be measured. The indentations must be small and fairly close together--typically from 50 microns to 1 mm. Figure 2.1 shows the two indentations separated by a fatigue crack; however, the gage can be used to measure strain on solid specimens. Since the two indentations are very close together, the diffracted patterns overlap and generate interference patterns on either side of the incident laser beam. If the distance between the indentations (d) changes, the interference fringes move, and this motion can be related to the displacement δd.

Indentations can be easily applied to the surface of a specimen with a Vicker's hardness tester which impresses a pyramidal diamond into the material. Figure 2.2 is a photomicrograph of two such indentations placed so as to measure displacement across a fatigue crack. The spacing between the indentations is 50 microns with each indentation approximately 17 microns along a side. This is a typical application; the indentations can be made smaller (but the interference pattern becomes dimmer) and can be located closer together or more widely spaced. The indentations are the actual gage, and they can easily be applied to polished specimens. The surface in Figure 2.2 is polished very well; a less careful polish that leaves scratches in the surface can be acceptable.

Techniques for making indentations (or in some cases wedge-shaped grooves), illuminating the gage, and recording and reducing the data and general operating procedures are well developed and are described in a review article [16] plus other papers [17-19].

The path difference between rays of light emanating from the two

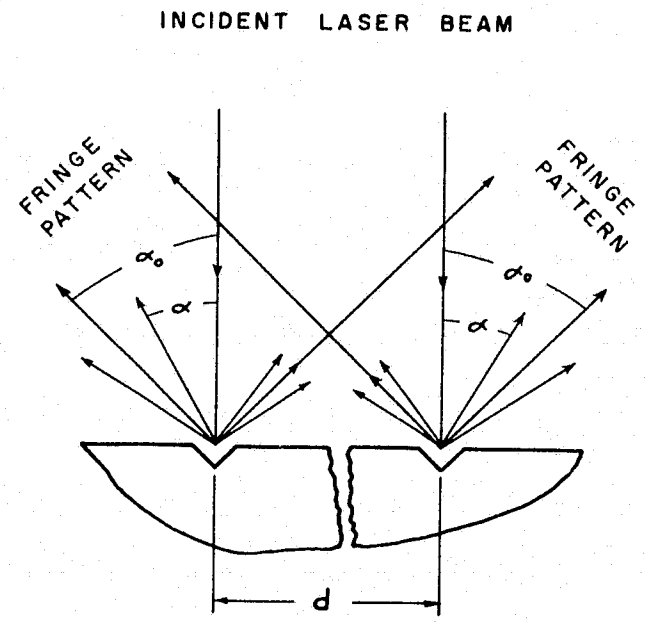

Figure 2.1 - Schematic of the interferometric displacement gage.

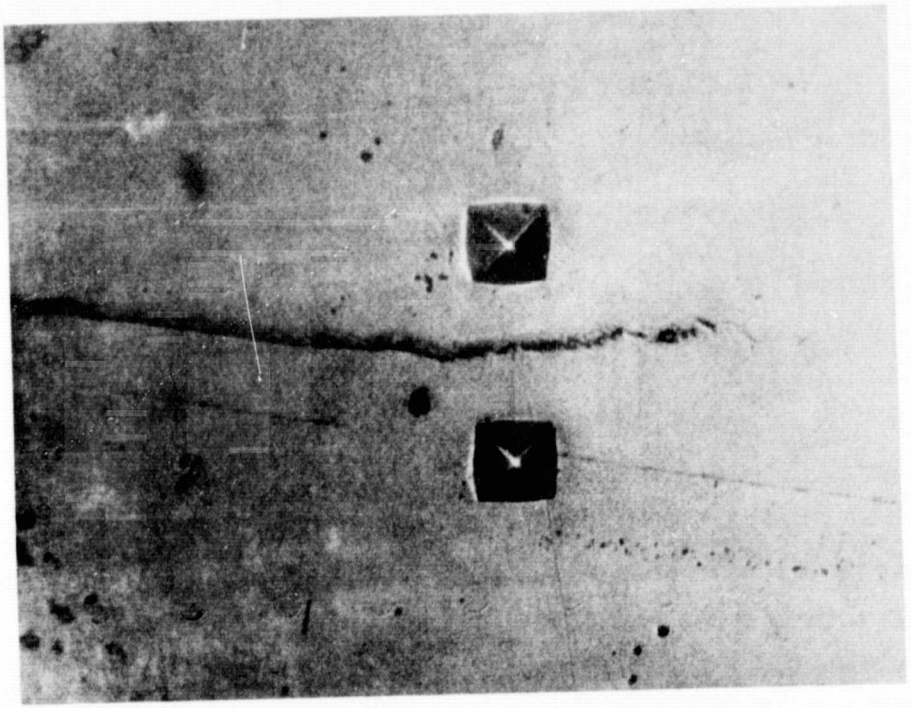

Figure 2.2 - Photomicrograph of two indentations 50 microns apart placed across a fatigue crack.

indentations is d sin α, where α is the angle from the normal incident laser beam to the rays in question (see Figure 2.1). Whenever the following relation is satisfied,

$$d \sin \alpha = m \lambda \qquad m = 0, \pm 1, \pm 2, \ldots \tag{2.1}$$

the light rays of wavelength λ interfere, constructively generating bright fringes. If one observes the fringe pattern from a fixed observation position, say α_o, while the indentations move relative to each other, the fringes move past this position and the relation between displacement and fringe motion δm is

$$\delta d = \frac{\lambda}{\sin \alpha_o} \delta m. \tag{2.2}$$

δm is the number of fringes or fraction thereof passing the observation position.

If the two indentations of Figure 2.2 move apart, the fringes move toward the incident laser beam. This is explained by equation (2.1), which shows that as d increases α must decrease. It is therefore convenient to define fringe motion toward the incident beam as positive corresponding to a tensile strain or displacement.

Fringe motion can be caused by rigid body motion as well as relative displacement. When the specimen moves parallel to its surface and along a line between the indentations (i. e., vertically for the indentations in Figure 2.2), one fringe pattern moves toward the incident laser beam and one moves away. Therefore, averaging the fringe motions eliminates the rigid body motion, and one should calculate displacement with equation (2.3):

$$\delta d = \frac{\lambda}{\sin \alpha_o} \left(\frac{\delta m_1 + \delta m_2}{2} \right). \tag{2.3}$$

This component of rigid body motion is present in every ordinary system for loading specimens, so that it is very important that it be averaged out. Other rigid body motions, e. g. one perpendicular to the specimen surface, are not averaged out and can lead to errors. In a carefully aligned testing machine, these components of rigid body motion can be made small, eliminating the need for further corrections.

Basically, the adjustment of the sensitivity of the technique lies in

the quantity δm in equation (2.2). The calibration factor $\lambda/\sin \alpha_o$ is typically about micron, so a fringe shift of $\delta m = 1$ corresponds to a displacement of 1 micron. Previous measurements have fallen into three categories based on the sensitivity of the fringe motion measurement:

1) Sensitivity of $\delta m = 0.5$, range of $\delta m = 10$ [15, 17, 18]: In this case, δm is measured by electronically monitoring the fringe pattern with a photomultiplier tube or photodiode and counting the fringes as they pass a fixed position.
2) Sensitivity of $\delta m = 0.1$, range of $\delta m = 5$ [15]: δm is monitored by following a given fringe with a photodiode mounted on a displacement stage. Sensitivity is determined by the sensitivity of the fringe maximum or minimum. Previous measurements were fairly crude; this approach could be improved to a sensitivity of $\delta m = 0.01$.
3) Sensitivity of $\delta m = 0.001$, range of $\delta m = 0.25$ [19]: Here one takes advantage of the linearity of the fringe pattern intensity in the region of $\frac{I_{max} - I_{min}}{2}$. This technique is amplitude-dependent, whereas the other two are not. It appears that this is near the lower limit of sensitivity of the IDG, but a sensitivity of 10^{-3} microns is likely to be more than required for macroscopic measurements.

Apart from the obvious advantage of small size, the IDG has some other advantages. It does not constrain the mechanical behavior of the specimen because the gage has zero stiffness. The frequency response of the gage is limited by electronic considerations and can be very high. The IDG can be used in hostile environments such as high temperature if the reflecting surfaces can be preserved. It is possible (and practical) to attach two small tabs of polished metal to materials like graphite or graphite-epoxy and form indentations in the tabs to make a gage.

The full potential of this measurement technique will not be realized until an instrument is developed that will produce a voltage output proportional to displacement. This can be accomplished with a computerized system for monitoring the fringe motion and reducing the data via equation (2.3). Initial development of such a system is the subject of this report.

3. FRINGE SCANNING SYSTEM

The plan for developing this displacement-measuring instrument was to transform the intensity of the fringe patterns into electrical signals which would be processed by a minicomputer. This approach gives maximum flexibility for arranging data reduction schemes for various applications. Some applications will not require a minicomputer system but can perform the data reduction with microprocessors or analog techniques. This section describes the hardware used in the instrument development.

3.1. Minicomputer System

The minicomputer has a 16-bit I/O board and 8-k memory. It is interfaced to a converter with 16 channels of A/D and 4 channels of D/A. Communication with the minicomputer is via a standard teletype. A single channel flexible disk is also attached, but this has been used only for software development, not data acquisition or processing. Economic constraints forced us to assemble this minicomputer system from components rather than purchasing a complete package.

3.2. Photodiode Arrays

Developments in optoelectronics over the past few years have produced small photodetectors in linear or two-dimensional arrays. An application of a linear array is position sensing; the 2-D arrays may well become the TV cameras of the future. The idea of using a linear array of photodiodes to monitor the fringe motion is attractive, but such an array turns out to be unsatisfactory because the aperture of the individual photodiodes is only slightly larger than the "speckles" appearing in the laser interference fringe pattern; thus a smooth representation of the fringe pattern is not obtainable.

A model RL-256C/17 linear photodiode array was obtained for evaluation from the Reticon Corporation, 910 Benicia Avenue, Sunnyvale, California, 94086. This array has 256 individual diodes, each with an aperture of 25 microns (1 mil) by 525 microns (17 mils) on 25 micron centers. This 6.3 mm long array is mounted on an 8.9 cm x 5.7 cm driver/amplifier PC board which is attached to a motherboard controller. The clock rate was set at 10 KHz, which means that a complete scan would take place at the rate of 40 Hz, i.e., displacement would be measured at 40 Hz if the minicomputer processing is fast enough.

These devices are used primarily for position sensing in which the position of an object is determined by its shadow falling on the array. The silicon photodiodes are usually driven to saturation in these applications, generating a useful "on-off" switch. The three main concerns prior to evaluating the device were sensitivity, linearity, and uniformity. The sensitivity of the RL-256C/17 is excellent; room lights drive it to saturation, and a fringe pattern from a set of indentations illuminated with a 5 mw He-Ne laser produces near-saturation at the intensity peaks. The saturation output is approximately 3 volts. Experiments with a uniform light source (incoherent) and neutral density filters showed that the uniformity and linearity of the diodes was acceptable.

Figure 3.1a is a scan of six fringes with the diode array, and Figure 3.1b is an expanded scan of one fringe. The pattern intensity, as measured by the peaks representing the output of each diode, should vary smoothly. The reason it doesn't is that the interference pattern has a speckled appearance because of the high degree of coherence of the laser, and these speckles are only slightly smaller than the aperture of the diode. Figure 3.2 is a photograph of a typical fringe pattern with an aperture drawn beside it; it readily shows the difficulty.

One cannot avoid this speckle problem by moving the scanner relative to the fringe pattern size. If the scanner is moved away from the specimen, the speckles become larger with respect to the aperture. If the scanner is moved closer, the speckles become smaller, but then one has only a few diodes per fringe, which makes fringe location imprecise. The diode array is unsuitable for this application.

3.3. Oscillating Mirror System

The approach here is to have the fringes impinge on an oscillating mirror which sweeps the pattern across a photomultiplier tube (PMT) with a slit aperture. The scanning mirrors selected are manufactured by General Scanning Inc., 150 Coolidge Avenue, Watertown, Massachusetts, 02172, and are their Model G-100 PD. This particular mirror has a built-in angle transducer which, when incorporated into the servo loop of their CCX-100 controller, gives precise position control. A scanning mirror is shown in Figure 3.3; the mirror is 6.3 mm x 6.3 mm. This mirror can rotate 20 degrees, and its response to a 300 Hz triangular input rotating it 15 degrees is excellent. In other words, given optimum minicomputer processing, displacement could be measured at 300 Hz.

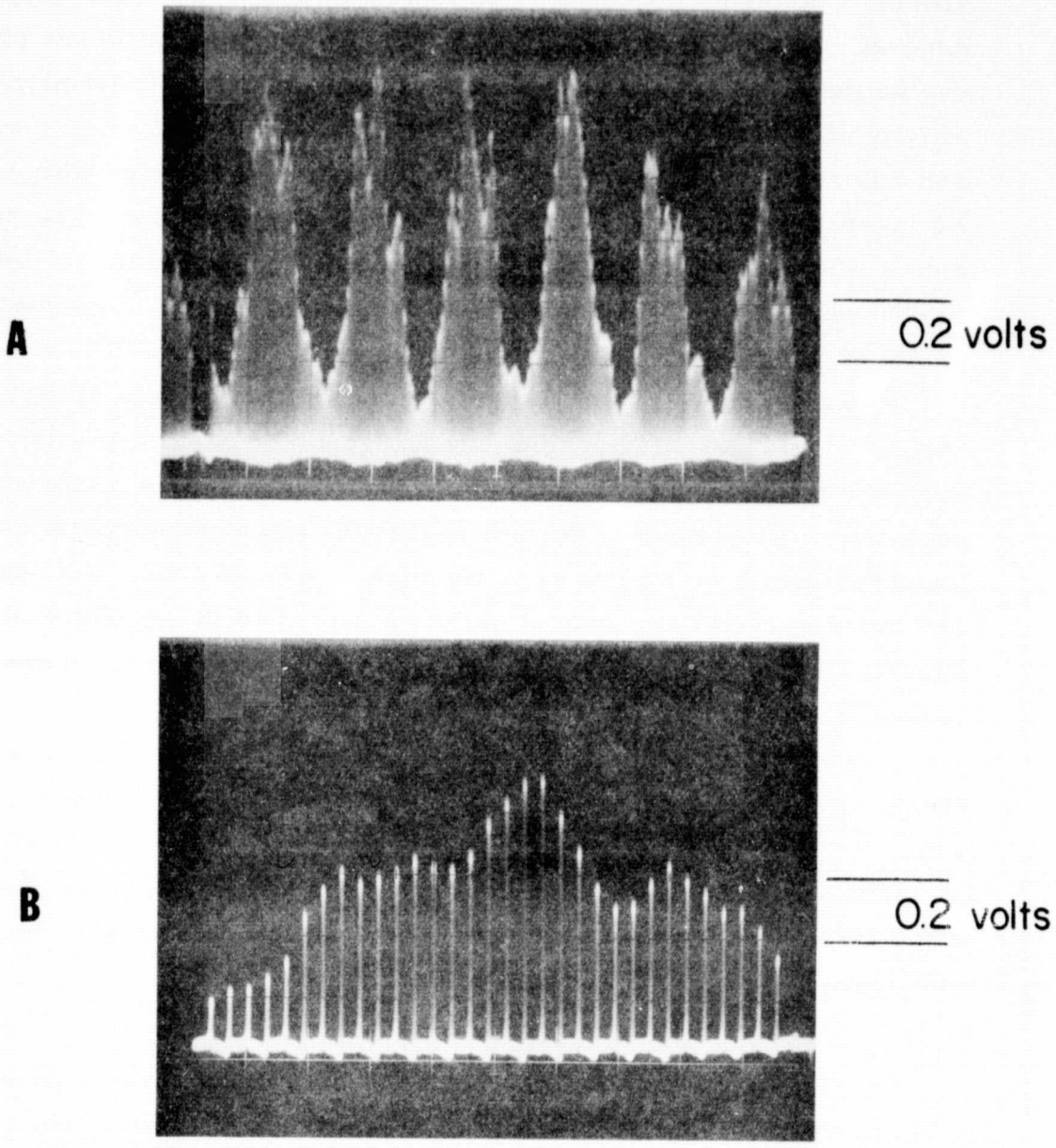

Figure 3.1 - Oscilloscope photograph of the output from a linear diode array. The upper photo shows the complete scan with 6 incident fringes. The lower figure shows one fringe expanded to illustrate the individual diode response.

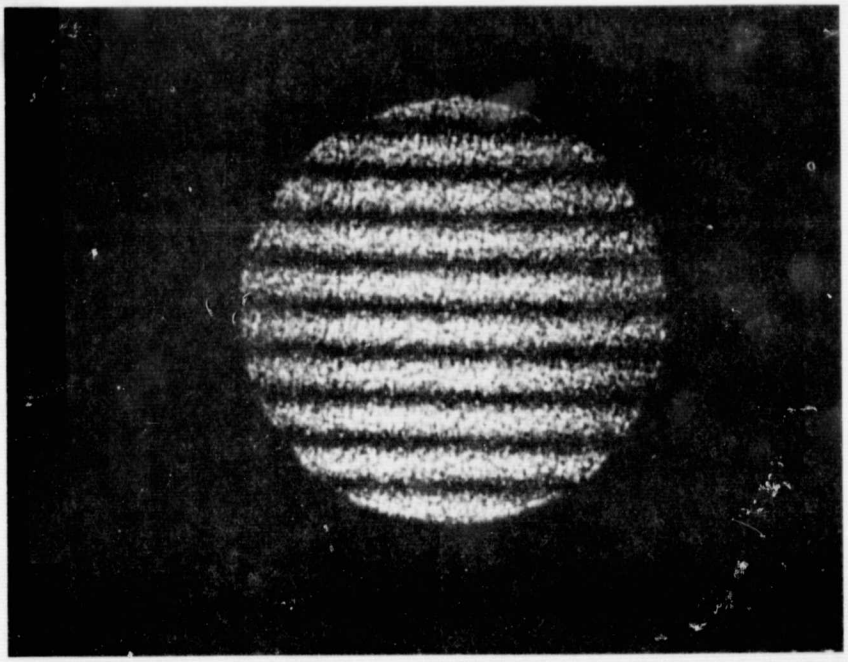

Figure 3.2 - Photograph of a typical fringe pattern showing its speckled nature. The photodiode aperture shown is scaled to show its size relative to the fringes.

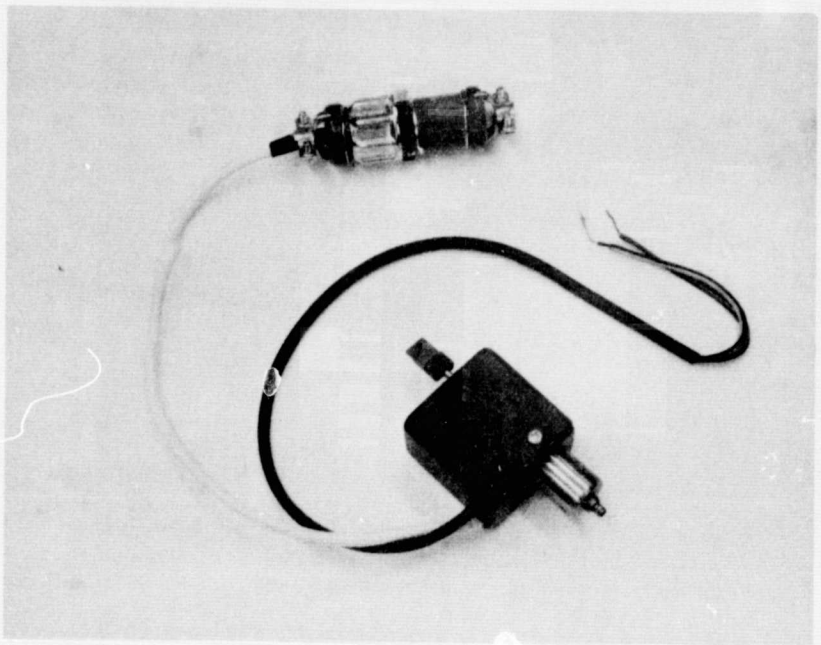

Figure 3.3 - Photograph of an optical scanner. The mirror is 6.3mm square. One lead is for the driving signal; the other is for the position transducer.

The first optical arrangement tried with the oscillating mirror is sketched in Figure 3.4 for one channel; two channels were used to average the fringe motion. The cylindrical lens could be moved back and forth along the optical axis, and its focal line was near the oscillating mirror. The lens collected all the emerging fringes and focused them on the small mirror. As the mirror oscillated, the entire fringe pattern was swept across the PMT slit. Moving the lens controlled the number of fringes impinging on the mirror and thus the precision with which fringes could be located. Calibration experiments revealed that rigid body motion of the specimen in a vertical direction (to be expected in a testing machine) was not averaged out. The reason was that it is very difficult to align both channels so that the optical paths are identical. Such an alignment would require that the distance from the lens to the oscillating mirror and the orientation of the lens be identical for both channels. Furthermore, both adjustable mirrors would have to have the same orientation with respect to the slit and the oscillating mirror. While such careful alignment could be attained for one setup, it is too difficult for laboratory use with various specimens.

A simpler and better system is illustrated in Figure 3.5. The alignment problems have been eliminated. Figure 3.6 is a closeup photograph of this system mounted on a "scanner board." The two oscillating mirrors, two photomultiplier tubes with their divider networks, and the end of the laser are shown. The laser is a 5 mw He-Ne type, and the photomultiplier tubes are operating with 1500 volts supply. Figure 3.7 shows the scanner board as mounted on a tripod in front of an Instron machine and also the power supply for the tube, the control circuit for the oscillating mirrors, and the minicomputer.

Figure 3.8 is a schematic of the electronics of the system. The mirror servo control is a type A-100 printed circuit board purchased from General Scanning Inc.; the unit with power supply and connectors was constructed at Michigan State University. The mirror-drive voltage from the minicomputer can be varied to adjust the angular scan of the mirror and thus control the number of fringes seen by the PMT. The PMT's put out a negative signal which must be inverted and amplified to be compatible with the A/D converter. A small op-amp circuit was constructed for this purpose, and a capacitor was included in the feedback loop of the op-amp

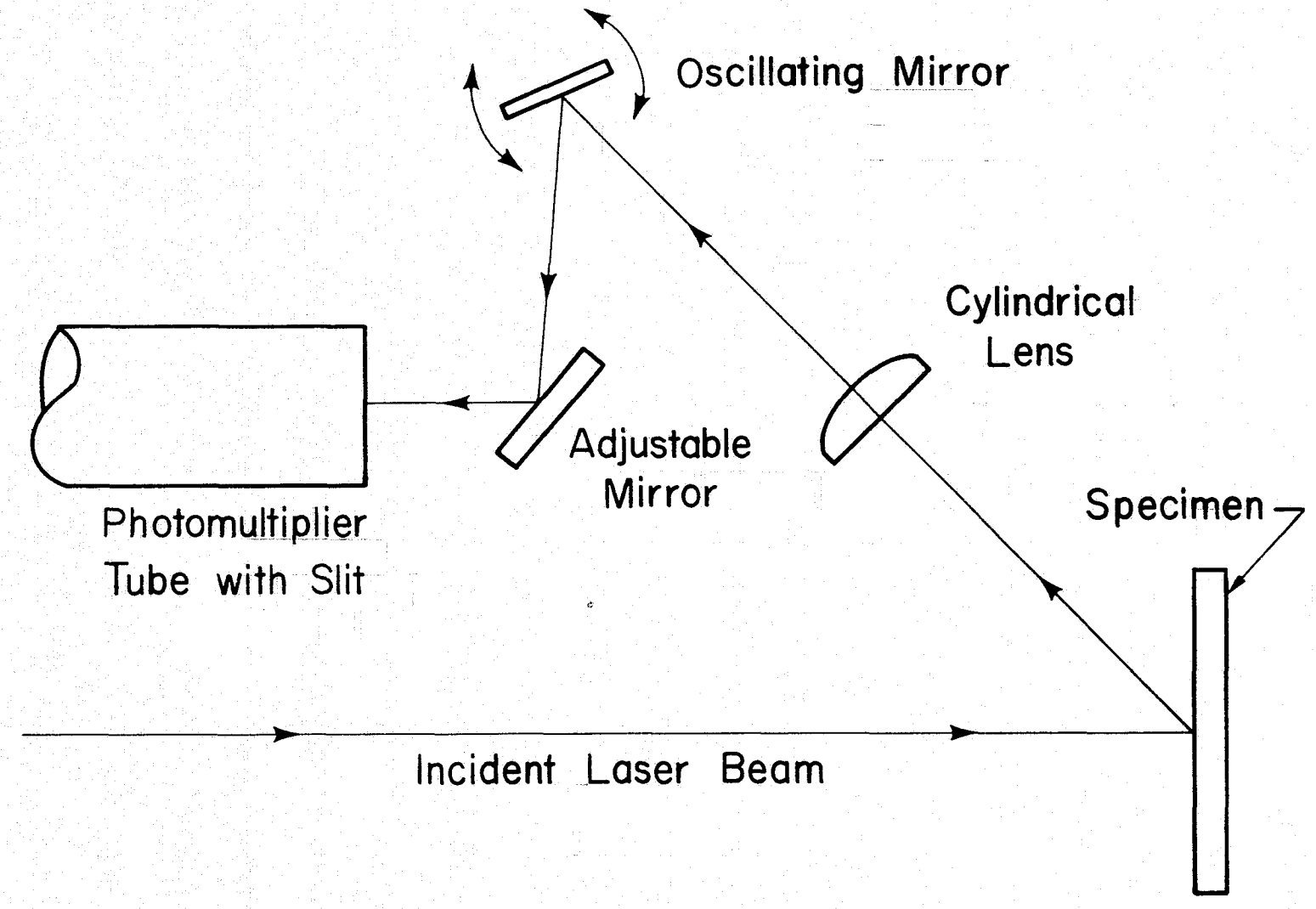

Figure 3.4 - Schematic of one channel of the first optical scanning system.

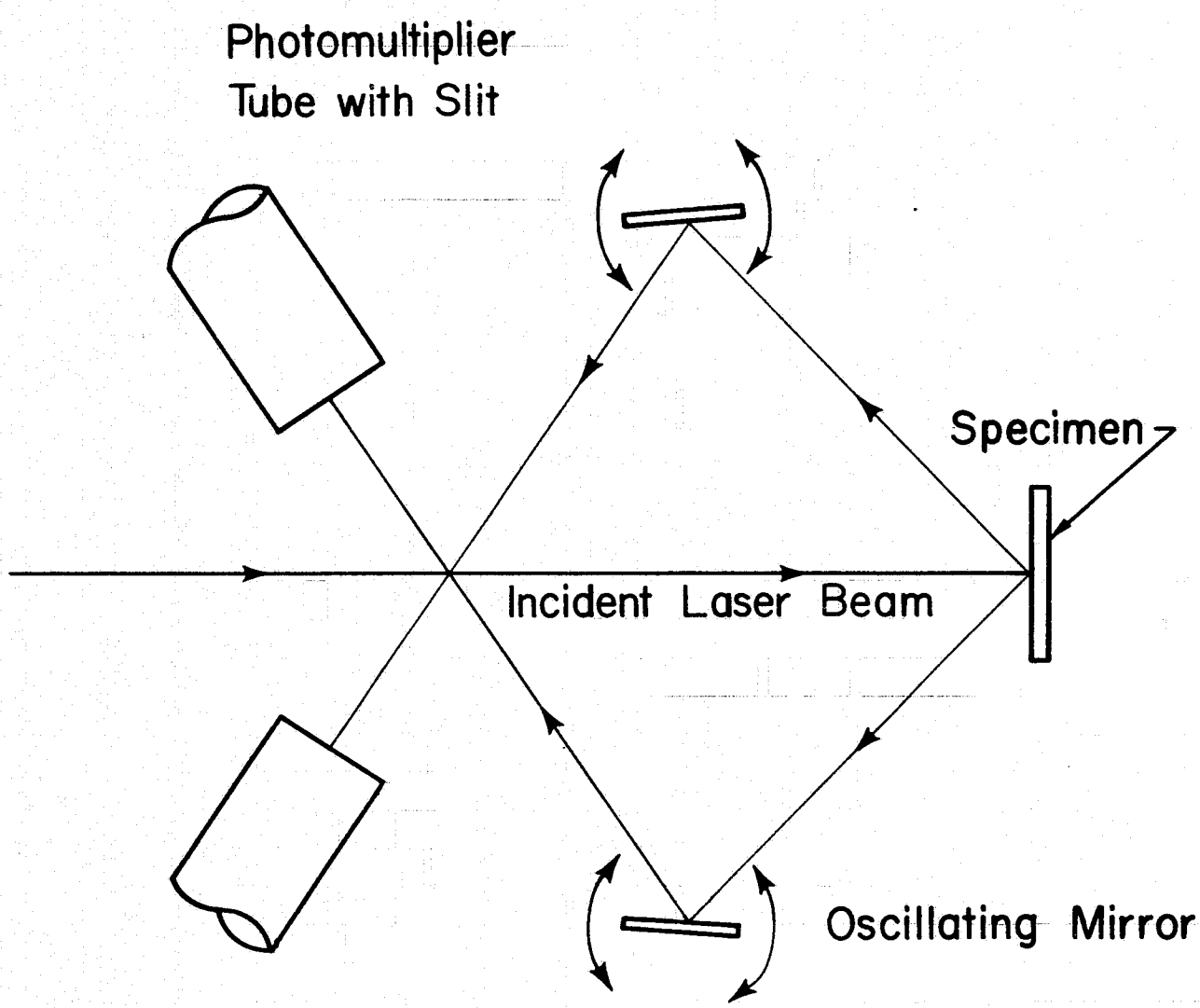

Figure 3.5 - Schematic of the final optical scanning system.

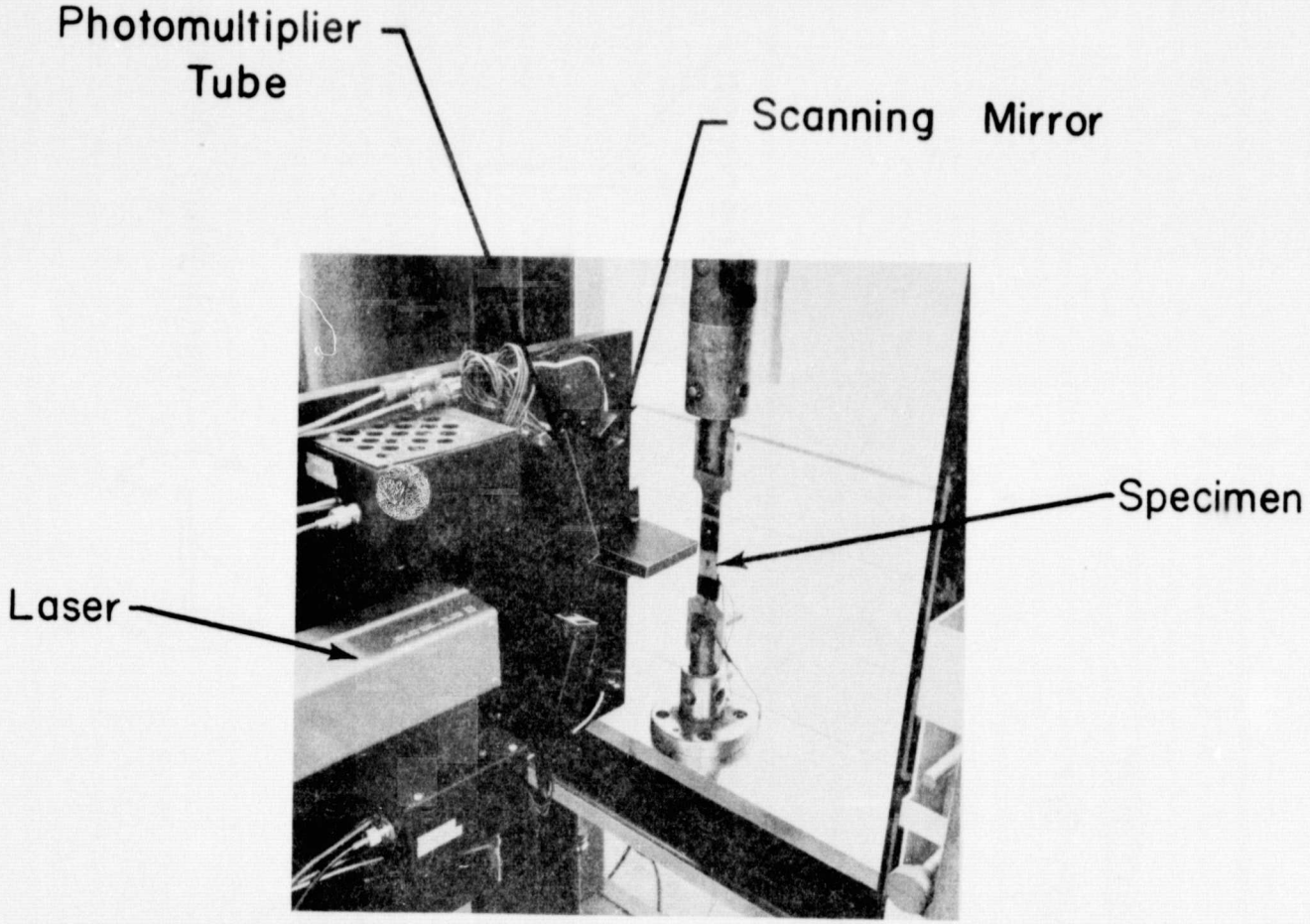

Figure 3.6 - Photograph of the fringe scanning system.

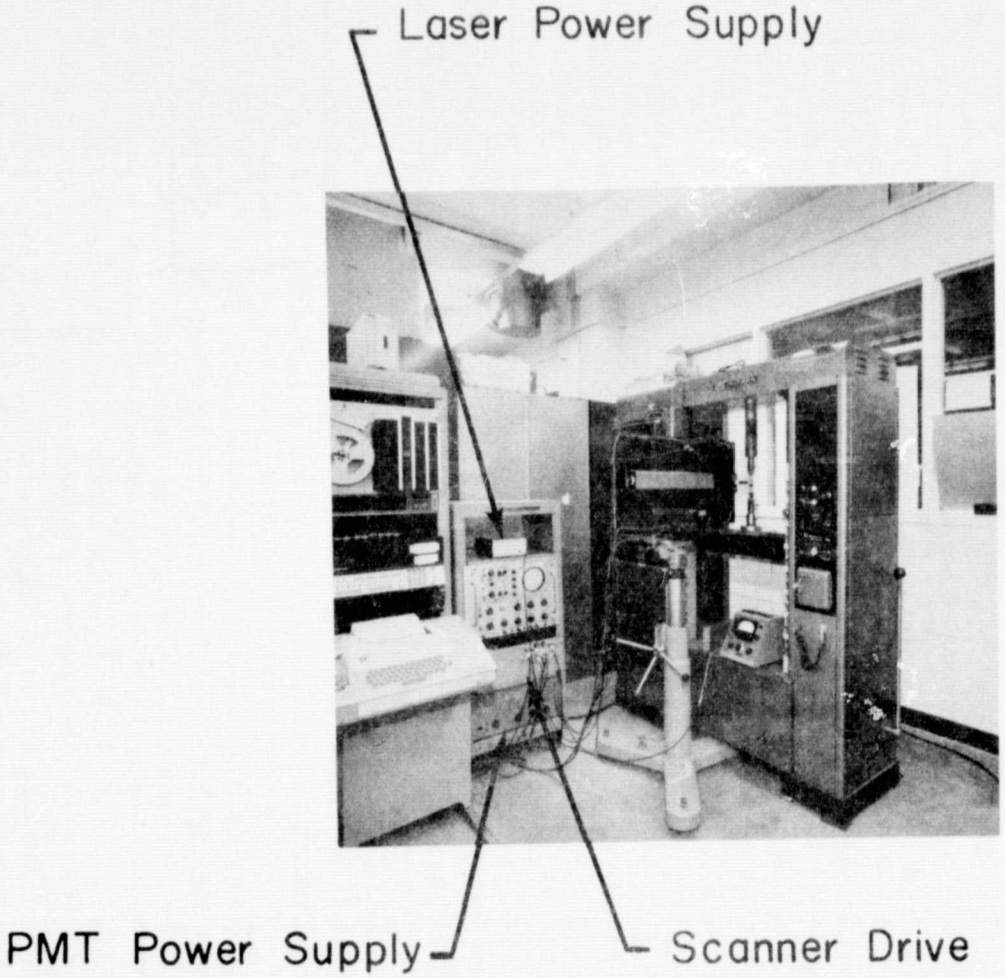

Figure 3.7 - Photograph of the displacement measuring instrument in front of a testing machine.

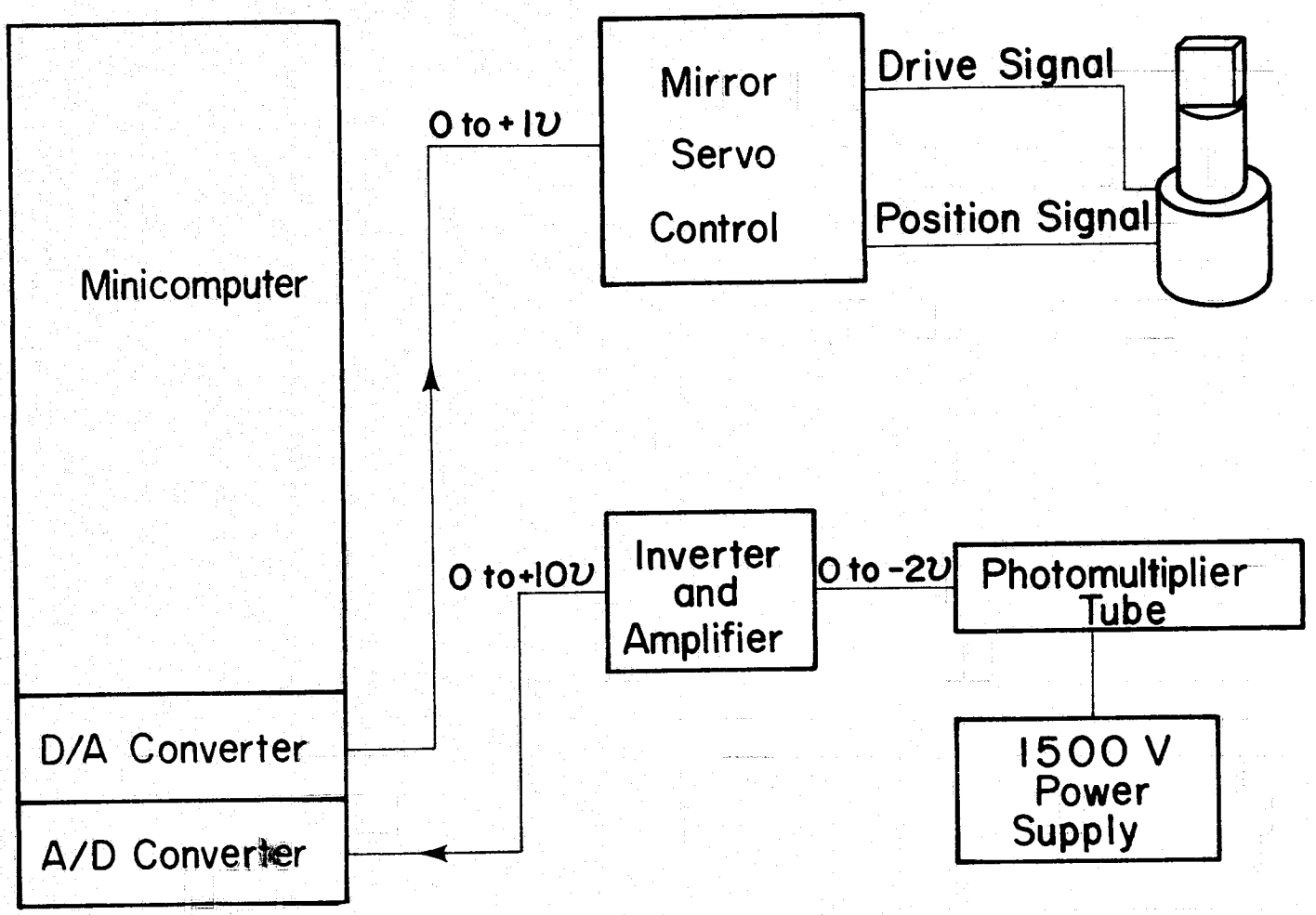

Figure 3.8 - Schematic of the instrument.

to filter the signal. This was necessary because the PMT signal had quite a lot of high frequency noise. The capacitor could be varied to match the scan frequency of the mirrors, and this proved to be quite convenient. A typical signal after it has been sampled 256 times is shown in Figure 3.9a and expanded in Figure 3.9b. A high quality signal like this means that simple compare statements can be used by the minicomputer to establish the memory locations of maxima and minima. Figure 3.10a shows both channels without filtering; the electrical noise is quite evident. Mechanical noise arising from motion of the scanner board and tripod is shown in Figure 3.10b.

Development of the optical, electronic, and mechanical systems to obtain good signals to present to the minicomputer was a major part of the effort on this project. Once proper signals are available, the displacement measurement is essentially a software problem. Software schemes for measuring small and large displacements are described in the following sections.

4. SMALL DISPLACEMENT MEASUREMENT

The scanner board was first used to measure very small displacements--less than one micron. Software, calibration procedures, and calibration results are presented in this section.

4.1. Software Program Description

To measure fractions of a micron, one must measure fractions of a fringe shift. The software developed scans both fringes, locates the maxima and minima of each fringe, and compares these locations for subsequent scans in order to measure fringe shifts. Once the fringe shifts have been computed, it adds them together and outputs the result as a voltage proportional to displacement. As presently existing, the program acquires the data during an experiment and outputs it after the experiment is over; it does not perform a real-time measurement.

The acquisition program is outlined in Figure 4.1. All controlling parameters are entered from the teletype. The starting position of the mirrors is controlled by output (via a D/A converter) voltages to the mirror controllers. This position is set when the mirrors are aligned so as to make the fringe patterns fall on the PMT slits. The patterns are initially positioned so that the slit is on one edge of the pattern because the mirror

A

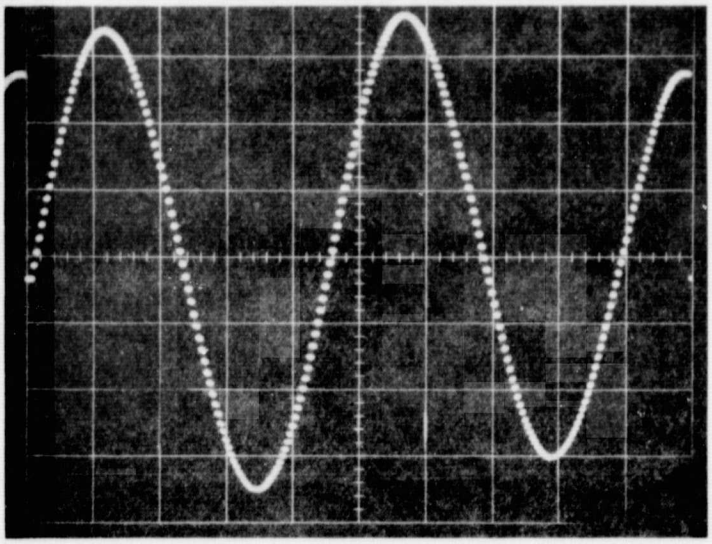

B

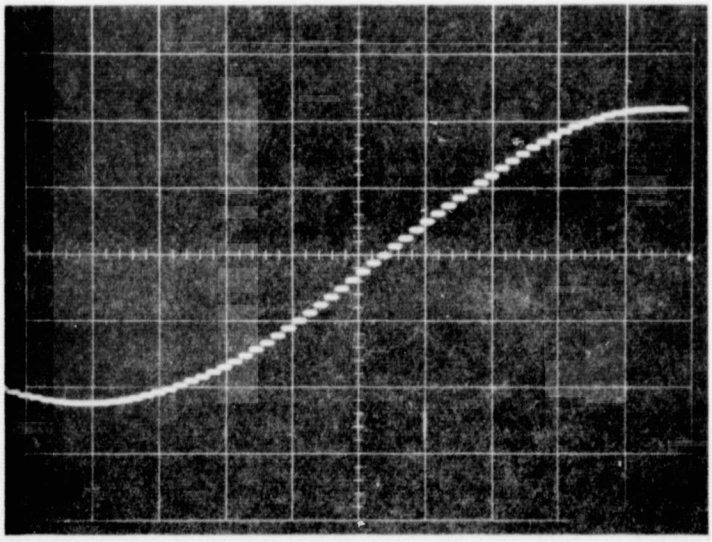

Figure 3.9 - Photographs of the sampled signal for two fringes from the fringe scanning systems. The lower photo is simply an expanded view of the upper one.

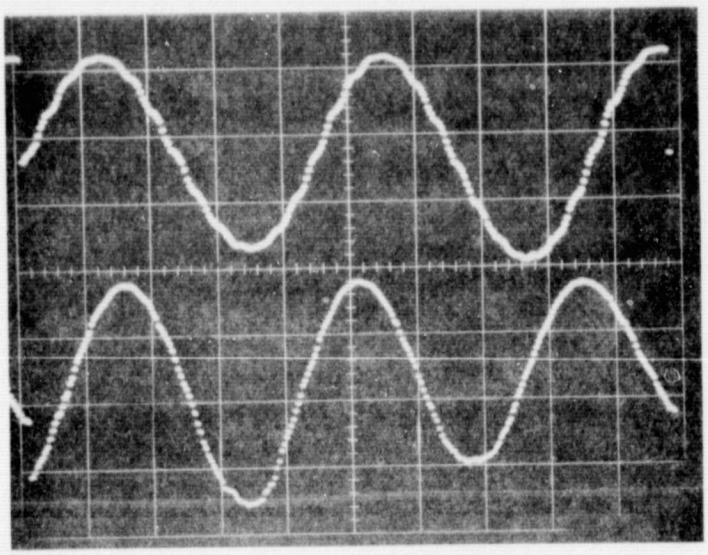

Figure 3.10a - Photograph of sampled fringe signals having electrical noise.

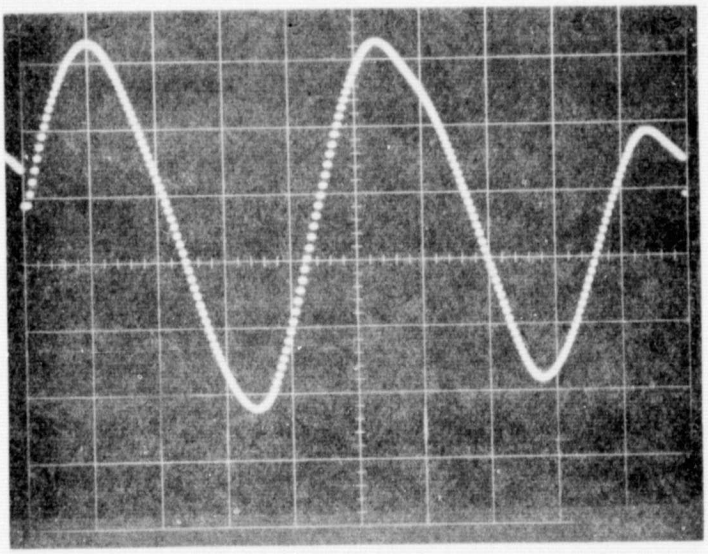

Figure 3.10b- Photograph of sampled fringe signal having mechanical noise.

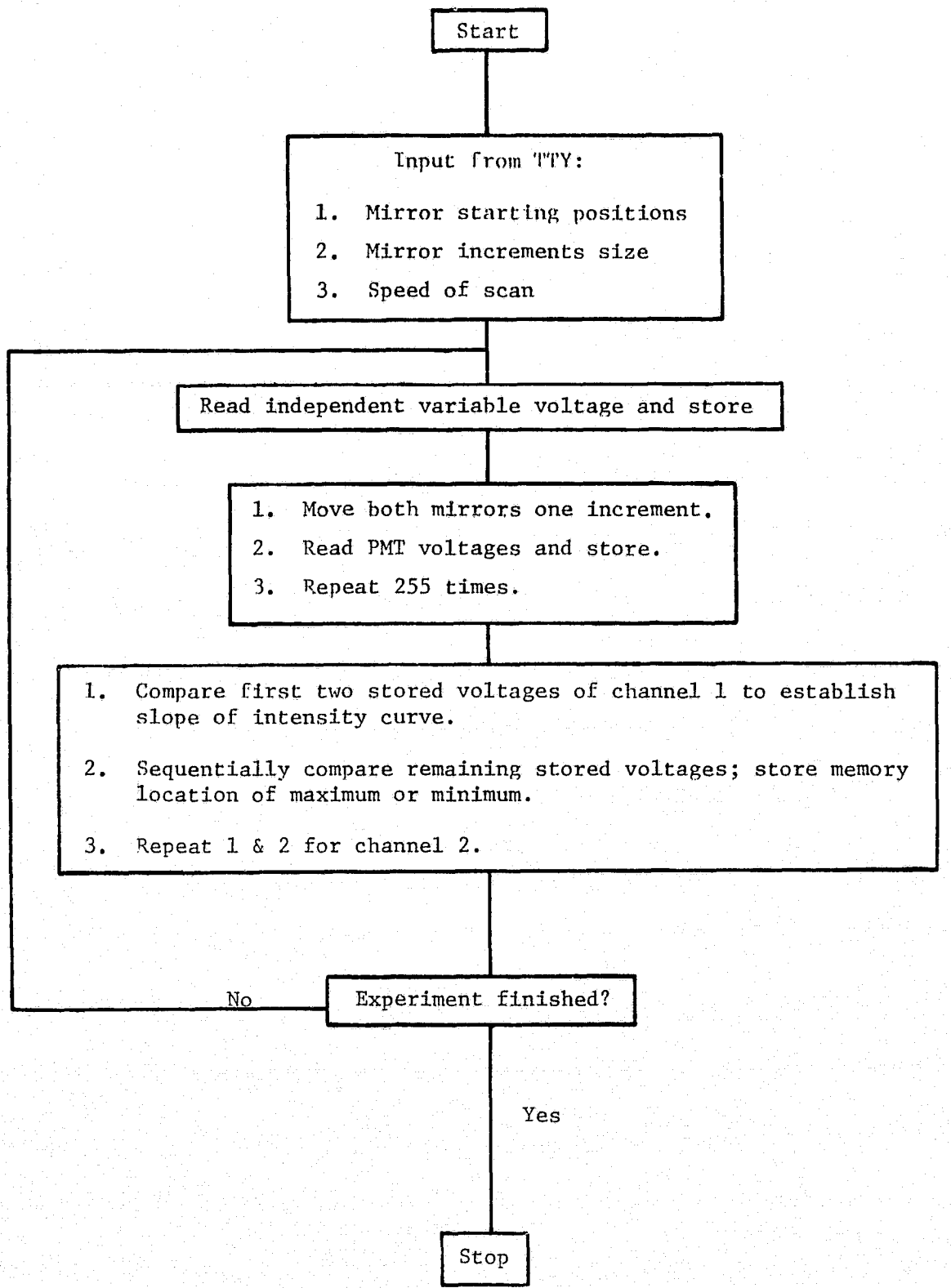

Figure 4.1 - Flowchart of data acquisition program.

driving wave form is similar to a periodic ramp function. The program is set up to scan the pattern in 256 increments; the size of these increments must be small enough that the total scan doesn't sweep the pattern off the PMT slit. The mirror is moved through its scan by simply incrementing the voltage applied to the mirror controller in a step-wise fashion 256 times and then returning to the starting voltage. There is a sharp transient applied to the mirror on the return to the original position and, when scanning at high speeds, the first few data points at the beginning of each scan are unreliable. The speed of scan can also be controlled, ranging from a maximum rate of 17 scans per second to approximately one scan per second. These adjustable parameters make it easy to adapt the measurement to the fringe pattern size (controlled by original indentations separation) and testing rate of various measurements.

This program is set up to measure one independent variable, e.g., voltage from a load cell, prior to each scan. After this voltage is read and stored, the mirrors then sweep the patterns across the PMT slit and the intensity versus angle information about the fringe pattern is stored temporarily in the form of voltage versus memory location.

After each scan, the data is processed to find the memory locations of the maxima and minima for each channel (see Figure 4.1). This is done so that the few memory locations (6-12) can be stored permanently instead of the 256 intensity voltages. Given a larger computer memory, this approach would not be necessary. Maxima and minima are located by stepping through the intensity voltages using simple "compare" statements. The first two data points of each scan are compared to establish the slope of the intensity curve. If this slope is positive, the next flex point will be a maximum, the next a minimum, etc. Each "data point" stored permanently consists of the independent variable voltage and the max/min memory locations for both channels. The measurement can be terminated by setting the level of the independent variable, the number of data points, or manually.

Following the conclusion of the experiment, the stored data is then processed and output to an X-Y recorder. Part of the total program consists of a single scan which scans the patterns, finds the maxima and minima, and computes (by subtracting memory locations) the spacing between fringes; this is then printed on the teletype. At present, this is used in

setting up for a measurement to adjust the spacing (via the variable mirror drive voltage) so that they are equal for both channels. This fringe spacing then becomes part of the calibration constant in equation (2.3) (along with a_o), which is also adjusted to the same value for each channel.

The compute and plot program (see Figure 4.2) takes as the zeroth fringe position the memory location of the first maximum of the first scan. The memory location of the first maximum of subsequent scans is then compared with this to establish absolute fringe shift. Maxima shifts of the two channels are added together to perform the averaging function in equation (2.3). This total shift is then output to the Y (or X) channel of an X-Y recorder and is proportional to displacement. When multiplied by $\lambda/2 \sin a_o$ and divided by the fringe spacing to obtain relative fringe shift, the absolute total fringe shift becomes equal to the displacement. This calibration is accomplished through the variable gain of the recorder. The total fringe shift is simply recorded as increments in a counter in the minicomputer; these are then output as voltage increments through the D/A converter. As currently set up, each increment corresponds to 0.156 volts; therefore,

$$\delta \text{ (microns/volt)} = \frac{\lambda}{2 \text{ (fringe spacing)} \sin a_o} \times \frac{1}{0.156 \text{ volts}} . \qquad (4.1)$$

Typically, with a fringe spacing of 125 memory locations (i.e., 2 maxima displayed in the 256 unit scan) and $a_o = 43°$, $\delta = 0.024$ microns/volt. Note that the 0.156 volts/increment is fixed in the minicomputer system, and for each measurement one must only obtain the original fringe spacings and angles to complete the calibration.

4.2. Measurand

A suitable method for generating measurands for small displacement calibration can be obtained by measuring strains in a uniformly stressed elastic member and converting these to displacements. The elastic member used was a simple tension aluminum specimen (4.5 mm x 25 mm in cross section) instrumented with a foil gage. It is shown mounted in a testing machine in Figure 3.6. The strain was measured with a strain indicator adjusted to 500 microstrain full scale. Two indentations 196 microns apart were placed on the polished specimen surface in the uniform stress section

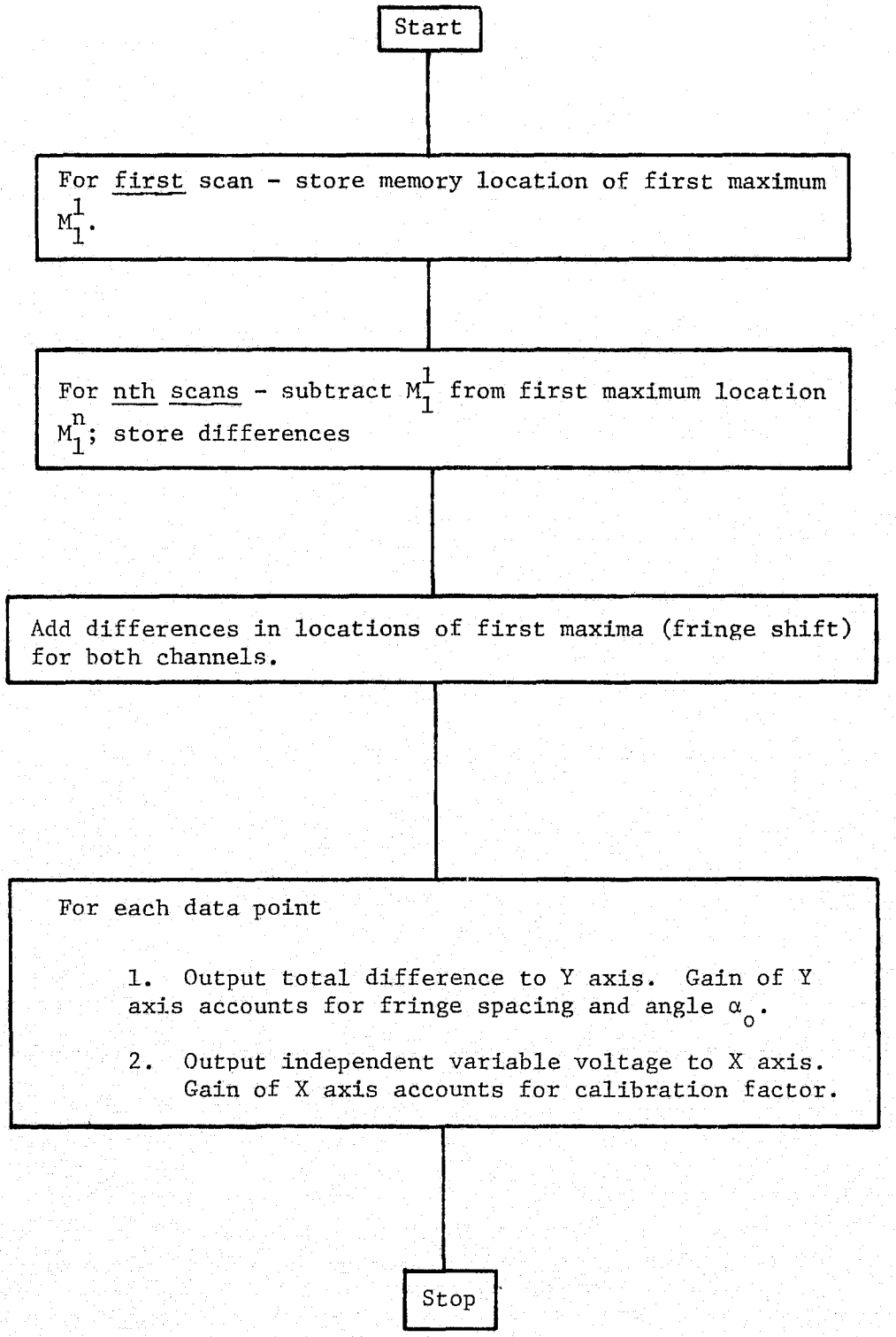

Figure 4.2 - Flow chart of compute and plot program.

of the specimen. The displacement between them is given by

$$\delta \text{ (microns)} = \text{strain} \times 196 \text{ microns.} \qquad (4.2)$$

The uncertainty in reading the strain indicator dial was 1 $\mu\epsilon$, so the relative uncertainty of displacement at 50 $\mu\epsilon$ (or 0.015 microns) would be 2 percent; at 500 $\mu\epsilon$ it would be 0.2 percent. The uncertainty of the gage factor of these gages is 1 percent, so it is estimated that the relative uncertainty of the measurand is no better than 1.5 percent for a total displacement of 0.1 microns. This is not an extremely accurate measurand; it was chosen for convenience. Strains would be measured more accurately with a large gage-length extensometer.

It should be noted that the purpose of the calibration tests was not only to verify the scanner board and minicomputer system, but to also demonstrate that this technique works with a typical testing machine in a general laboratory environment. The fact that this optical technique can accommodate the rigid body motions of a specimen in an ordinary testing machine and does not require special fixturing or isolation is very important.

4.3. Calibration Results

The first set of calibration results are presented in Figures 4.3 and 4.4. These calibration tests were computed manually, i.e., for each data point the location of the maxima and minima were printed on the teletype and the fringe shifts of the first two maxima computed. This was done to check for variation in fringe spacing and to get a "feel" for the data behavior. Figure 4.3 shows the five individual displacement tests, and Figure 4.4 gives the same data with average values ± one standard deviation being plotted. Figure 4.5 shows results for a series of increasing, then decreasing, displacement tests. These results show that the instrument measures these small displacements quite well; instrument specifications are given in the following section.

Figure 4.6 is a plot of one of the calibration tests showing the displacement computed from each channel separately. Channel 2 is the lower one. As the calibration specimen is loaded, it moves down, and this downward rigid body motion of the fringes on Channel 2 counteracts the upward fringe motion toward the incident laser beam due to tensile strain. The opposite is line for Channel 1 so that Channel 1 shows a lot more fringe motion than Channel 2. But, when averaged, the correct displacement is obtained.

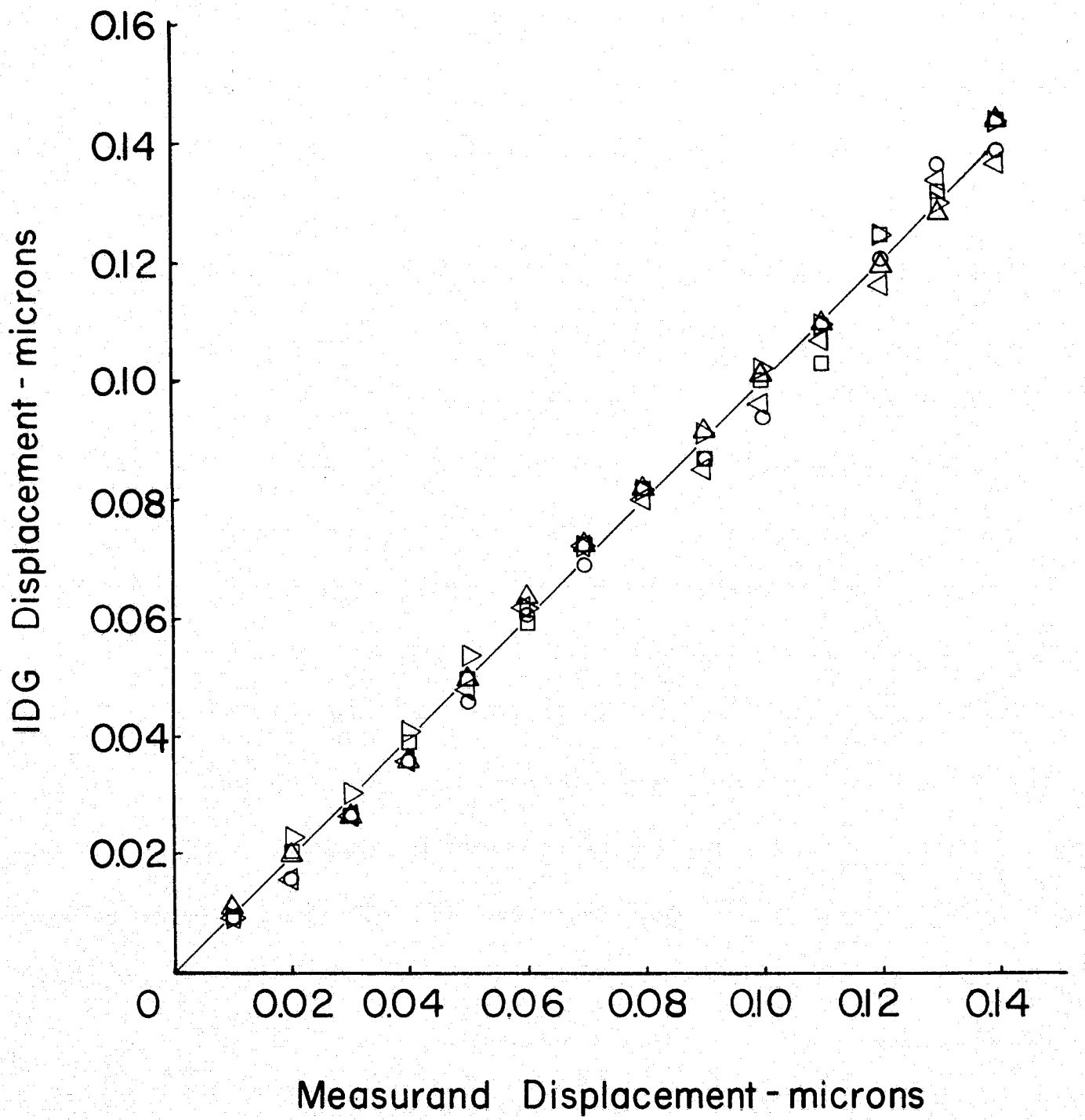

Figure 4.3 - Results of 5 calibration tests.

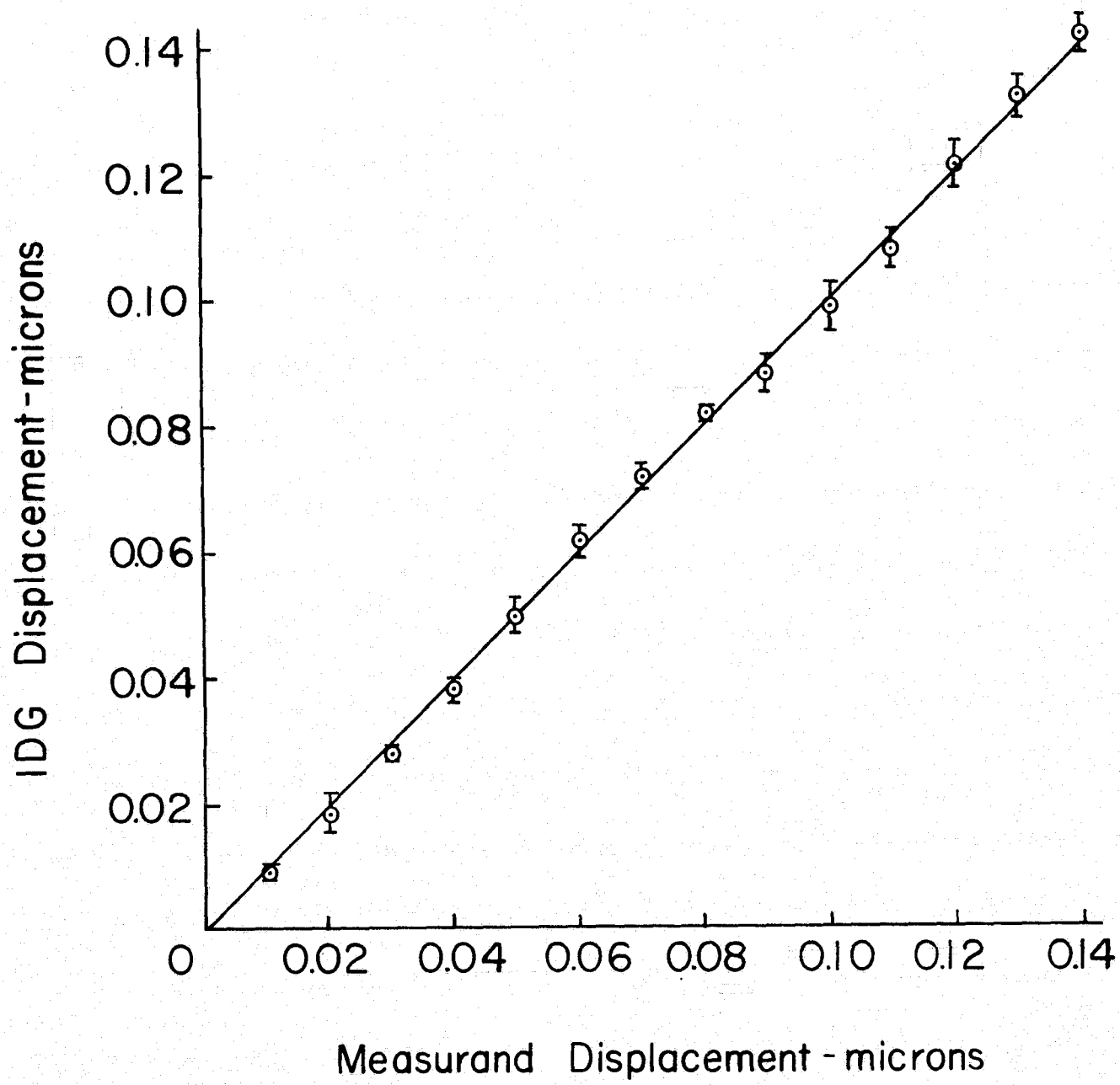

Figure 4.4 - Average results of 5 calibration tests. Vertical bars denote ± 1 standard deviation.

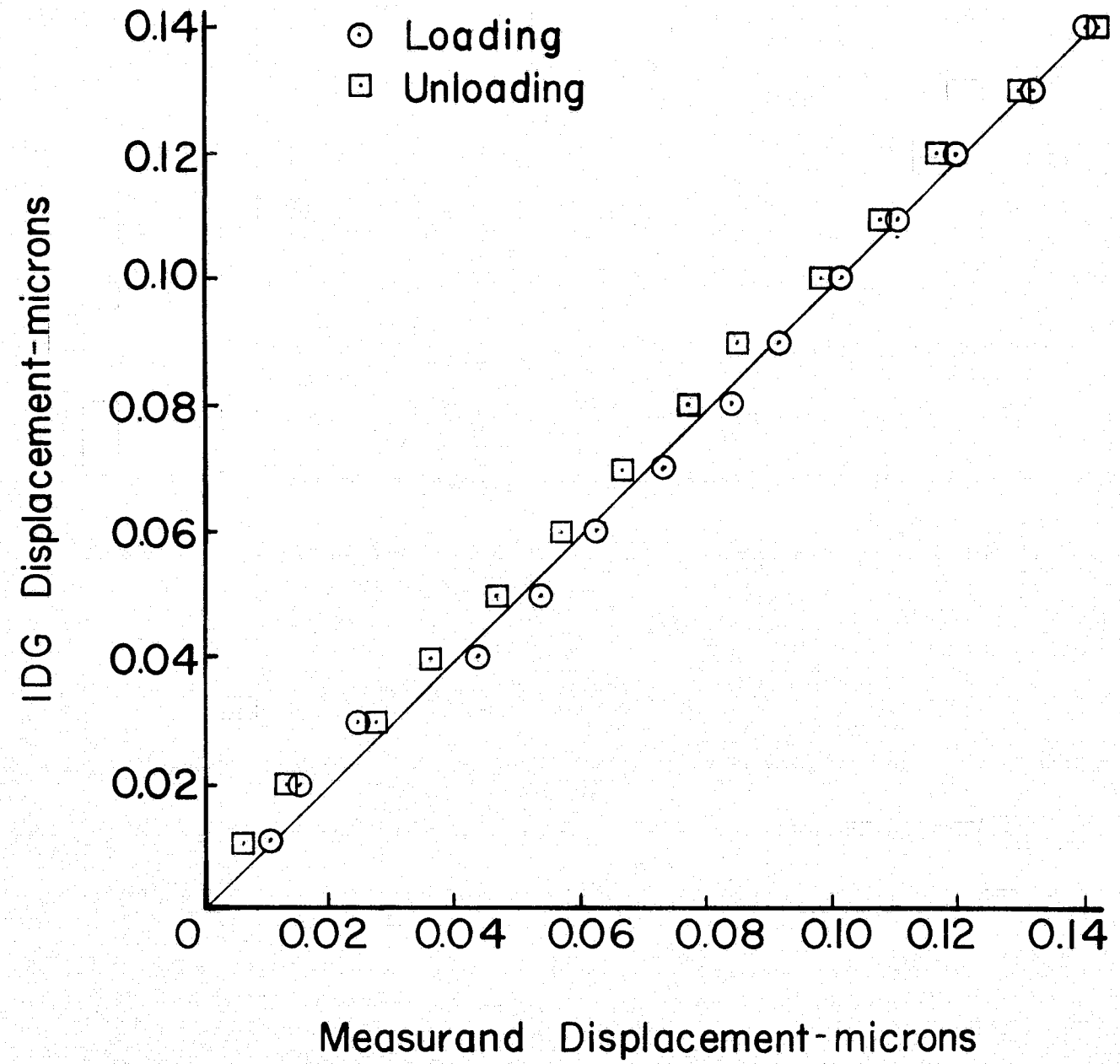

Figure 4.5 - Average results of 5 calibration tests in which the displacement was increased, then decreased.

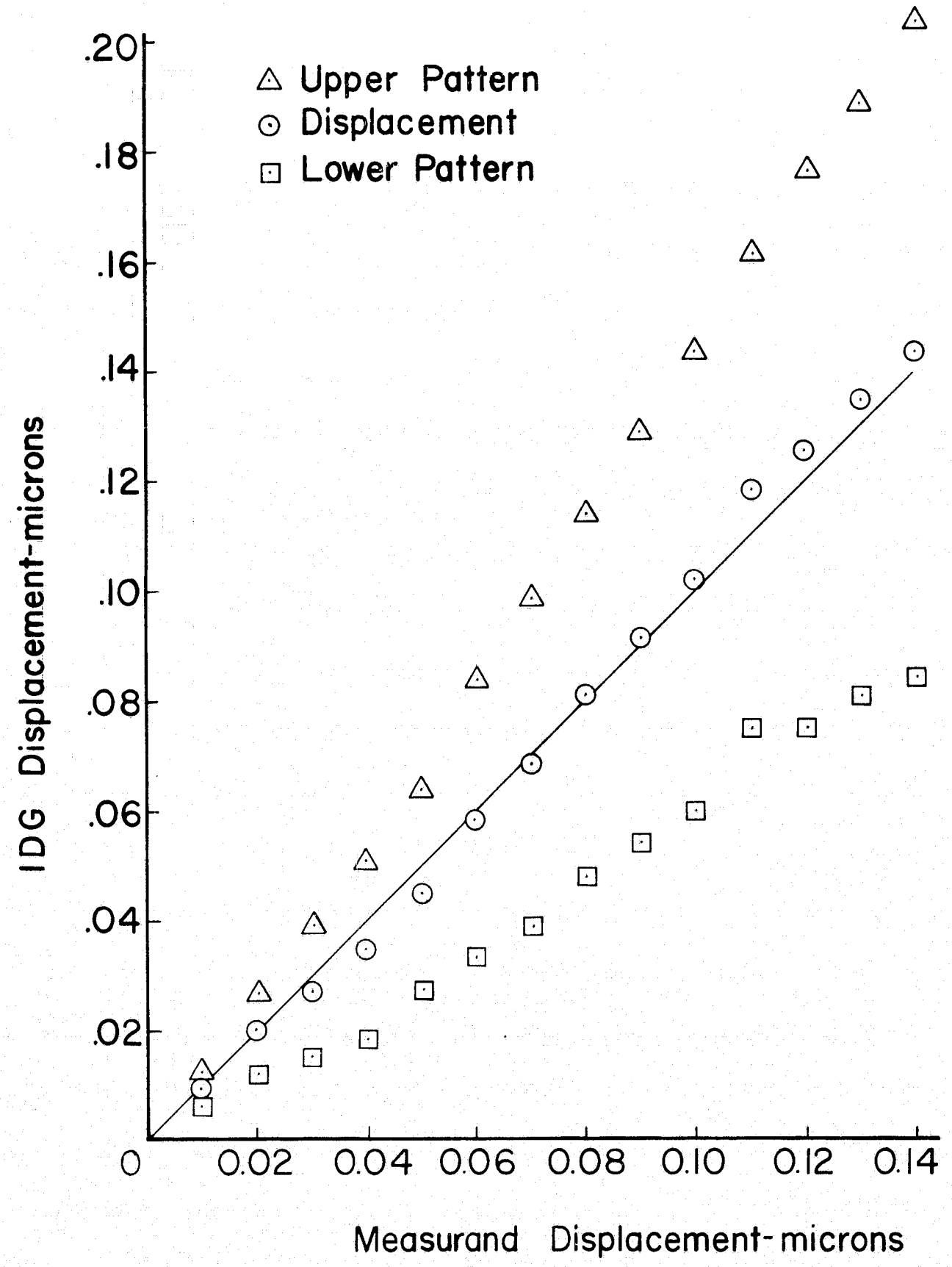

Figure 4.6 - A calibration tests showing the displacement associated with each fringe pattern.

When the plotting feature is used, the results are as shown in Figures 4.7 and 4.8 where 24 and 100 data points respectively are taken during the calibration. Each data point does not correspond to an increment in fringe maximum shift in Figure 4.7, but to an integer number of increments. In Figure 4.8 most of the vertical steps between points correspond to one memory location shift. The scatter accentuated in Figure 4.8 arises from the fact that when one scans a stationary (no specimen displacement) fringe pattern, one doesn't always get exactly the same memory locations for maxima and minima. The electrical and mechanical noise has been reduced to the point that these locations differ no more than 1 memory location, e.g., the first maximum might be located at either memory location 55 or 56. This effect is of course most important in small displacements.

4.4. Instrument Specifications

Based on the calibration results, the following specifications can be written for this displacement-measuring instrument.

4.4.1. Resolution--0.004 micron

This is controlled by the number of memory locations between fringe maxima. For these tests, that number was about 125. So the smallest displacement detectable is:

$$\delta = \frac{1/125}{2} \frac{\lambda}{\sin \alpha_o} = 0.0037 \text{ microns}.$$

Resolution could be improved by enlarging this number, but unless the stability of the fringe transducer system were improved, the uncertainty in locating the maxima and minima would increase and no advantage would be gained. For most measurements of mechanical displacement, this resolution is more than adequate.

4.4.2. Range--0.14 micron

The range specified is for these calibration tests, which are computed using the first maximum only. Software can be developed to account for a new "first" maximum entering the scan, and the range can be extended. It appears to be only a software problem to extend the range of the measurement to 3 mm.

4.4.3. Error Band--± 5 percent

This is based on full scale and includes linearity and repeatability.

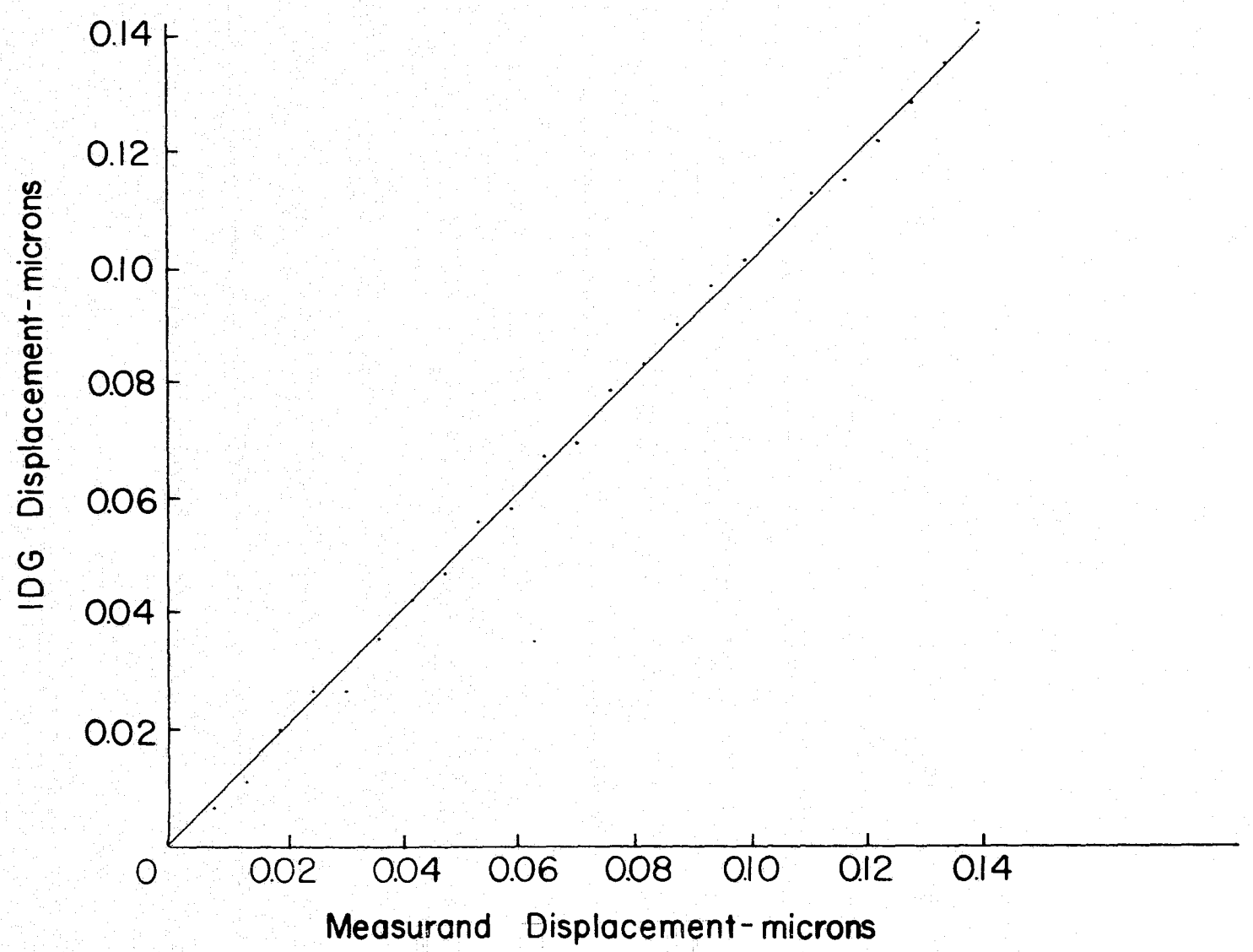

Figure 4.7 - A calibration test consisting of 24 points and using the plotting routine.

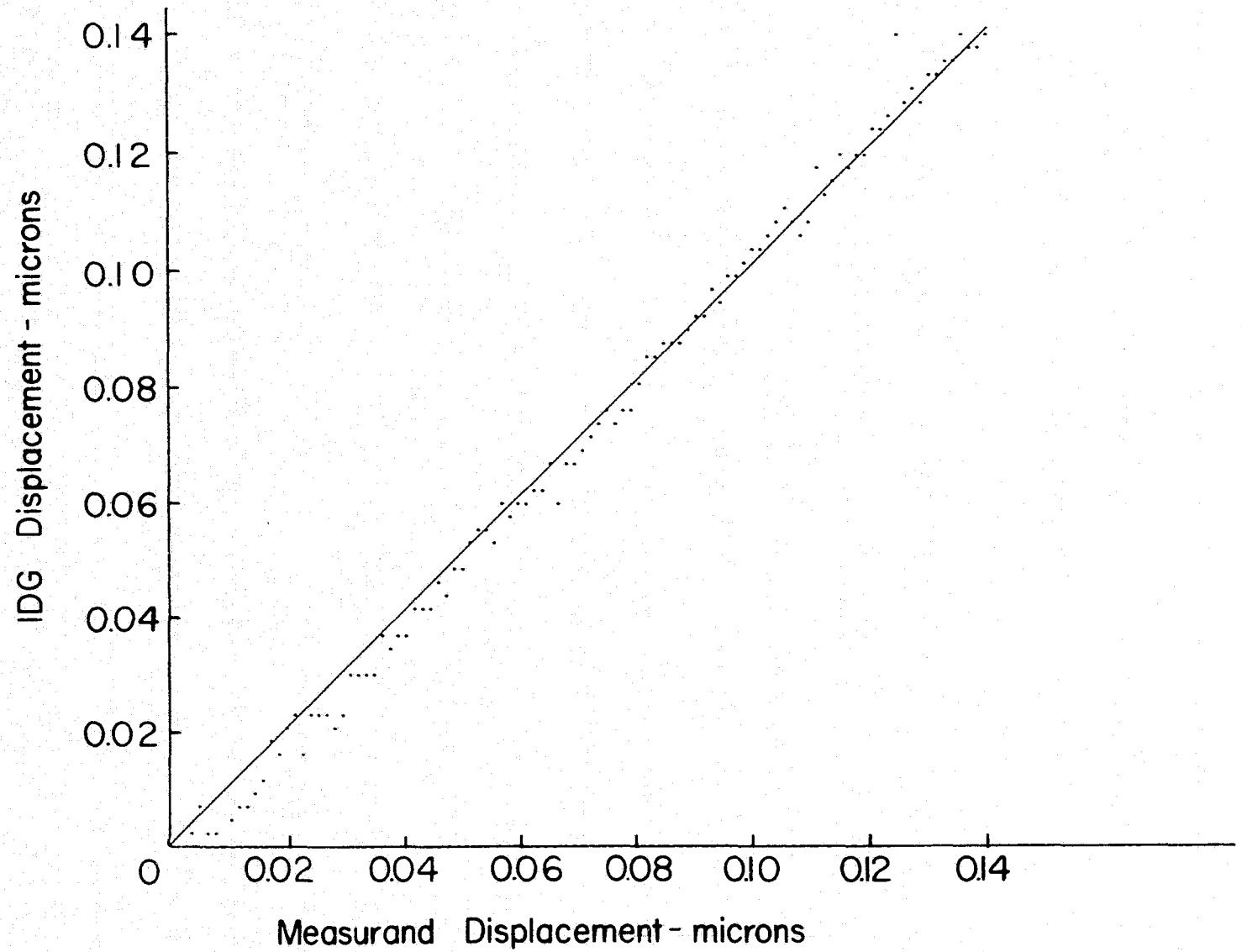

Figure 4.8 - A calibration test consisting of 100 points and using the plotting routine.

4.4.4. Hysteresis--± 1.5 percent

This is based on the average values of five loading and unloading tests.

4.4.5. Sampling Rate--17 points per second

This could be improved by about a factor of 2 by acquiring all the data without processing it for maxima locations.

4.5. Recommended Software Development

A program should be written to account for new "first maxima" entering the fringe pattern scan from either direction (i.e., increasing or decreasing memory location). This would extend the range of the measurement. A program of this nature appears straightforward, but is likely to take a fair amount of time. Note that this is strictly a software problem; no changes in the scanning system would be required. Once this is accomplished, the small displacement technique will be more useful in the laboratory.

Several software improvements can be suggested, but the most useful one would average the fringe shifts of all maxima and minima in a scan, not just the first maximum. This would probably lower the error band and hysteresis, smooth out data like that in Figure 4.8, and be a significant improvement.

5. LARGE DISPLACEMENT MEASUREMENT

Large displacement refers to values greater than 10 microns or so. The system for making this measurement is considerably simpler than the one for small displacement and is described in this section.

5.1. Software Program Description

Here it is not necessary to measure small fractions of a fringe shift, so the program can simply arrange to count the fringes as they pass the PMT slits. Moveable or oscillating mirrors are not required, though they were used simply to direct the fringe pattern onto the PMT slits. The hardware for this kind of measurement is the same as used to measure small displacements.

The program is described schematically in Figure 5.1. The PMT's sense the increasing and decreasing voltages as the fringes pass over the tube slit. Voltages V_n are measured by the A/D converter and compared by the program to a reference voltage V_N; when this difference exceeds a

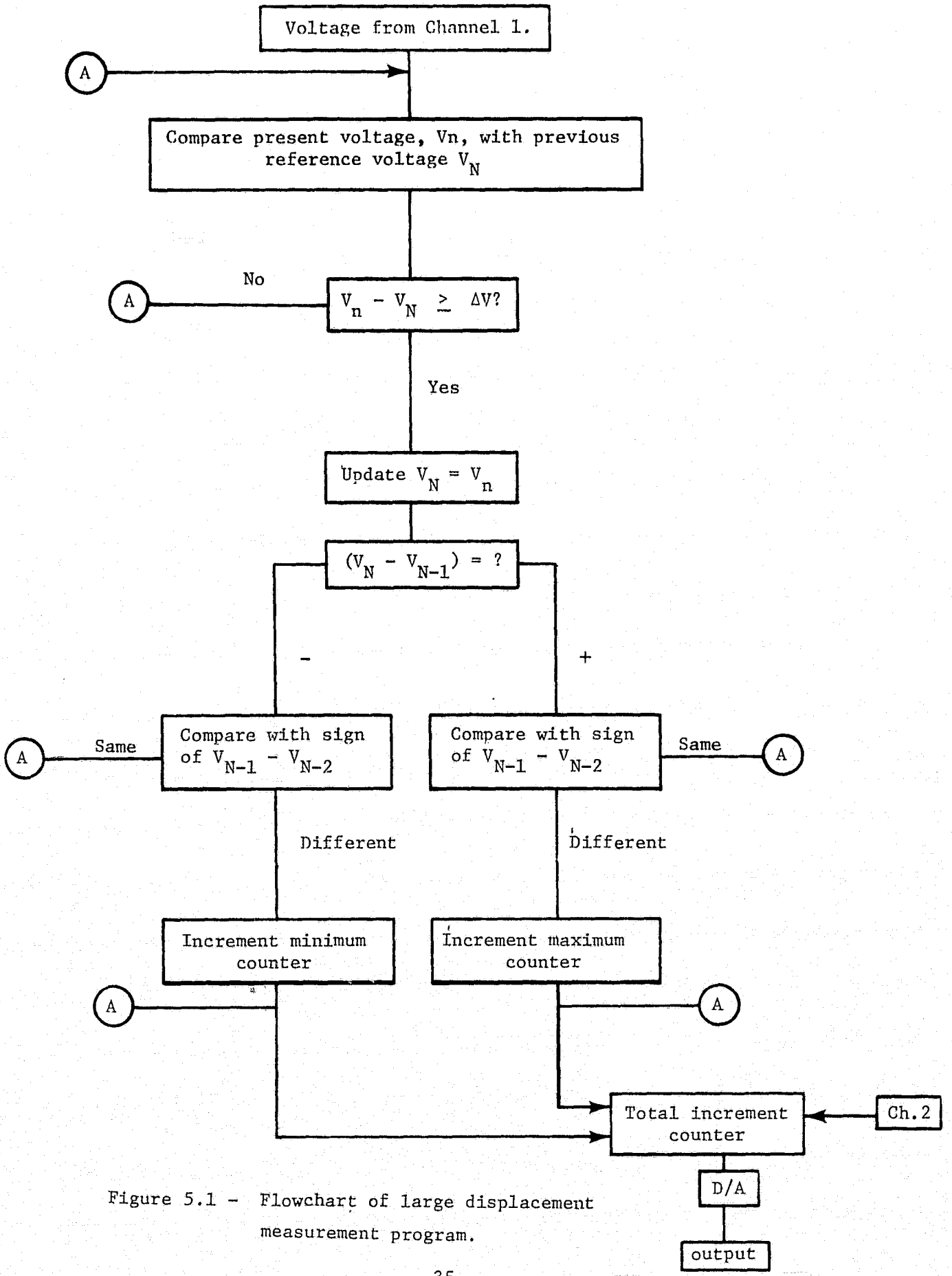

Figure 5.1 - Flowchart of large displacement measurement program.

certain voltage increment, ΔV, the reference voltage is updated. This new reference voltage is compared with the previous reference voltage $(V_N - V_{N-1})$ to determine whether it is larger or smaller. The sign from this comparison is then checked against the sign from the last comparison $(V_{N-1} - V_{N-2})$ to see if it is the same; if not, then a maximum or minimum in voltage has been observed. The program thus establishes the number of maxima and minima for both Channels 1 and 2 and adds these together into a total output count that is proportional to displacement.

The purpose of using for comparison only voltage data that exceeds previous data by ΔV is to reduce the effects of electrical noise in the system. From Figure 3.9 one can see that the voltage differences are very small in the neighborhood of a flex point and electrical or mechanical noise could lead to false counts. This same problem exists in the small displacement technique and accounts for some of the scatter in Figure 4.8; here it can easily be eliminated.

The output counter increments every time a maximum or minimum is recorded by either Channel 1 or 2. The resolution of this measurement is then:

$$\delta_{min} = \frac{1/4\ \lambda}{\sin \alpha_o},$$

or, with typical values, approximately 0.23 microns.

This program at present does not account for direction of fringe motion, so it can only be used to measure unidirectional displacements. However, a more complicated program can be developed to account for this.

5.2. Measurand

A measurand for large displacements can be obtained with a micrometer head attached to a translation stage (see Figure 5.2). The micrometer head has a resolution of 2 microns. The device used is augmented with an LVDT for analog output. Two polished aluminum tabs are attached to the fixed and moveable parts of the stage. A single indentation is placed on each tab; when the stage is closed, these indentations are approximately 160 microns apart. When the stage is opened, the largest displacement that can be measured is limited by the size of the laser beam incident on the indentations. In this setup, when the indentations were approximately 700 microns apart, the beam was too narrow to produce a

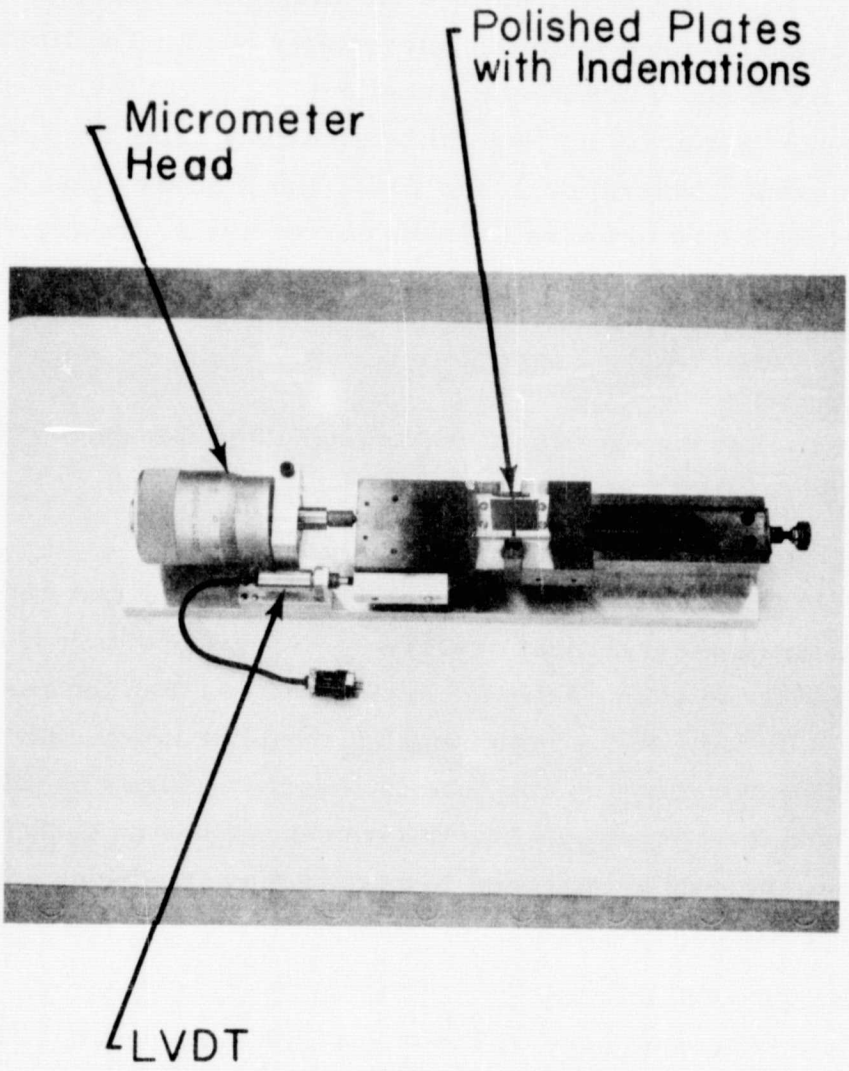

Figure 5.2 - Translation stage for large displacement calibration.

bright pattern. Calibration tests were run with a maximum relative displacement of 400 microns; the fringe patterns were very bright at a total separation of 560 microns.

5.3. Calibration Results

Figure 5.3 shows the calibration results for five separate tests with the measurand obtained from the micrometer head. The linearity and reproducibility of the calibration is excellent.

Figure 5.4 presents five calibration runs using the LVDT to record the measurand. Calibration of the LVDT itself showed that it was nonlinear, hence the slight bow to the calibration curve; again, the reproducibility is excellent. The stepwise output of the IDG is not discernible on this scale of measurement.

5.4. Instrument Specifications

The following specifications are based on the above calibration results.

5.4.1. Resolution--0.25 microns

This is established by the four inputs to the output counter. If one added two more channels that observed a different portion of the fringe pattern and fed those counts into the output counter, then the resolution would be cut in half, i.e., to 0.12 microns. It would be fairly easy to do this with the moveable mirrors and computerized system simply by moving each mirror back and forth to sample two different positions on each fringe pattern. This approach could be extended to sample more positions and further refine the resolution.

5.4.2. Range--400 microns

This is limited here by the size of the laser beam. The beam could be expanded with a lens to increase the range. When the separation between indentations becomes on the order of 3 mm, the fringes become so closely spaced that they are roughly the same size as the laser speckles; this limits the range to 3 mm.

5.4.3. Error Band--± 1 percent

This is based on full scale and includes linearity and repeatability.

5.4.4. Hysteresis--was not evaluated

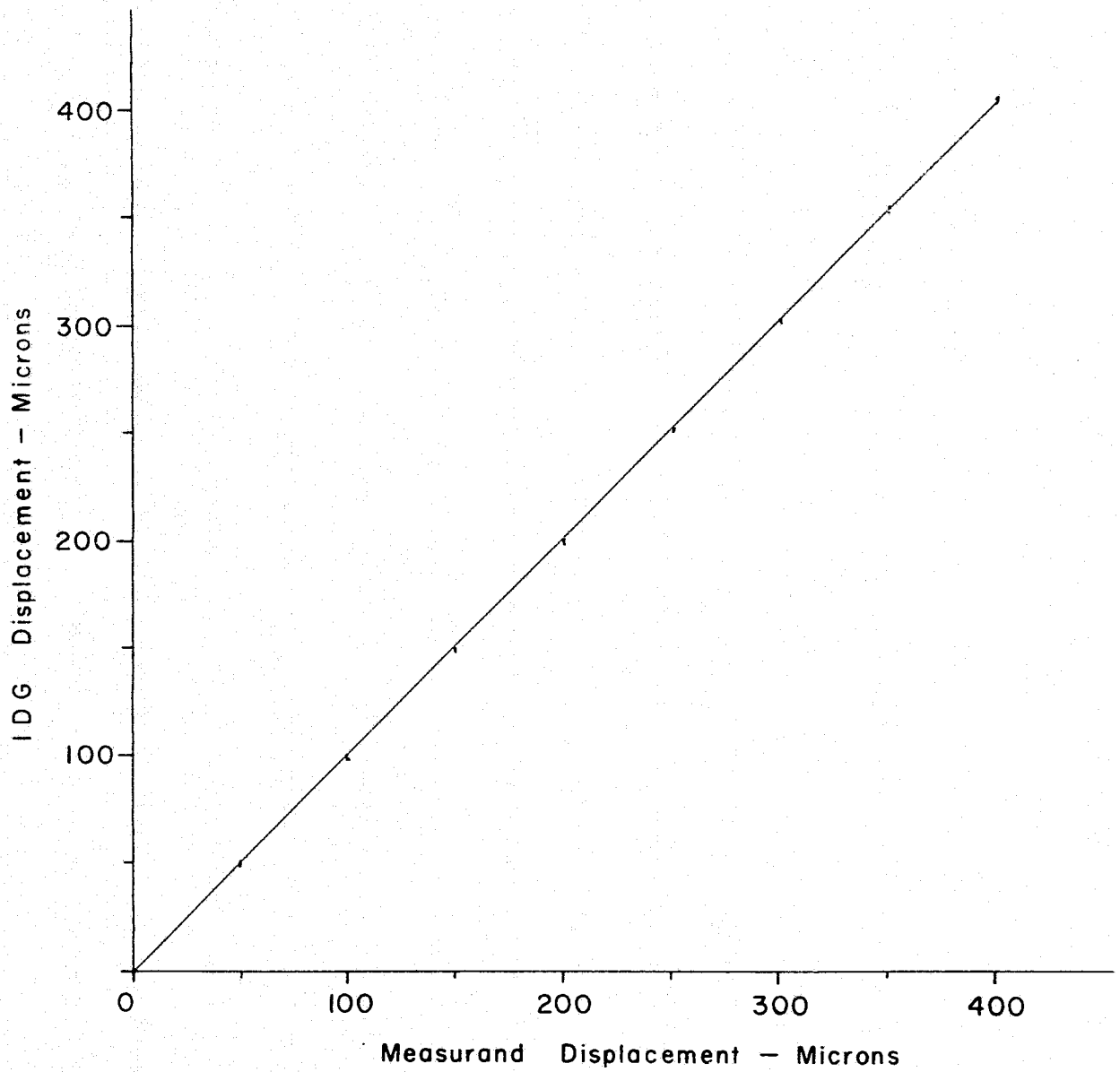

Figure 5.3 – Results of 5 calibration tests as recorded by X-Y plotter. Measurand was obtained from micrometer head.

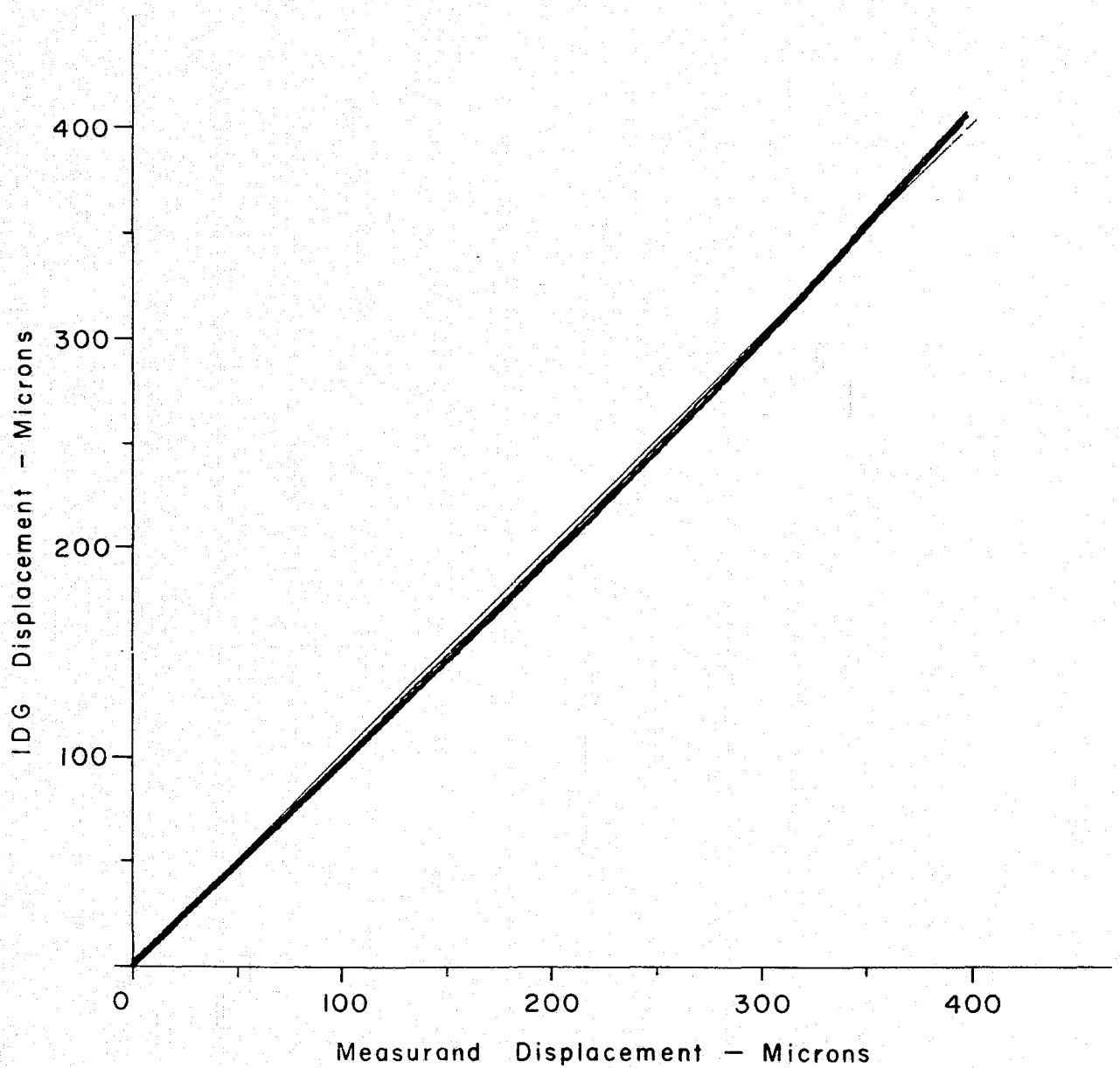

Figure 5.4 – Results of 5 calibration tests. Measurand was obtained from LVDT.

5.4.5. Sampling Rate--~ 2400 points per second

The maximum sampling rate with the present setup was not measured, but was computed to be 2400 points per second.

5.5. Recommended Software Development

A program should be developed to account for the direction of fringe motion of both Channels 1 and 2 and decrement the output counter for negative fringe motion. The system could then be used for cyclic displacement measurements. One way to do this is to have the mirrors move to sample two positions on a fringe pattern. Then, simply by inquiring which position had seen the most maxima and/or minima, one could ascertain the fringe direction. This approach would not only account for decreasing displacement, but would halve the resolution by counting twice as many fringes.

Given the direction-sensing feature,. this instrument could find widespread use in the laboratory because of its range and sensitivity.

6. INTERMEDIATE DISPLACEMENT MEASUREMENT

It appeared useful to evaluate the instrument as it currently exists for displacement measurement with a range of 10 microns. The small displacement technique cannot cover this range, so the large displacement technique was used.

6.1. Measurand

A good specimen for generating displacements in this range is a center-cracked tension specimen. If the geometry is within certain specifications, the displacement at the center of the crack can be computed from knowledge of the applied load.

A 3.0 inch (7.62 mm) by 1/8 inch (0.32 mm) specimen of Type 2219 aluminum was prepared with a center crack 0.010 inch (250 microns) wide and 0.5 inch (1.27 mm) long electro-machined perpendicular to the load axis. Indentations were placed on each side of the center of the crack and were located 300 microns apart. The specimen was loaded in a testing machine and the displacement measured with the large displacement technique.

6.2. Calibration Results

The results of a typical calibration test are given in Figure 6.1. The resolution of approximately 0.25 microns is quite evident there. The

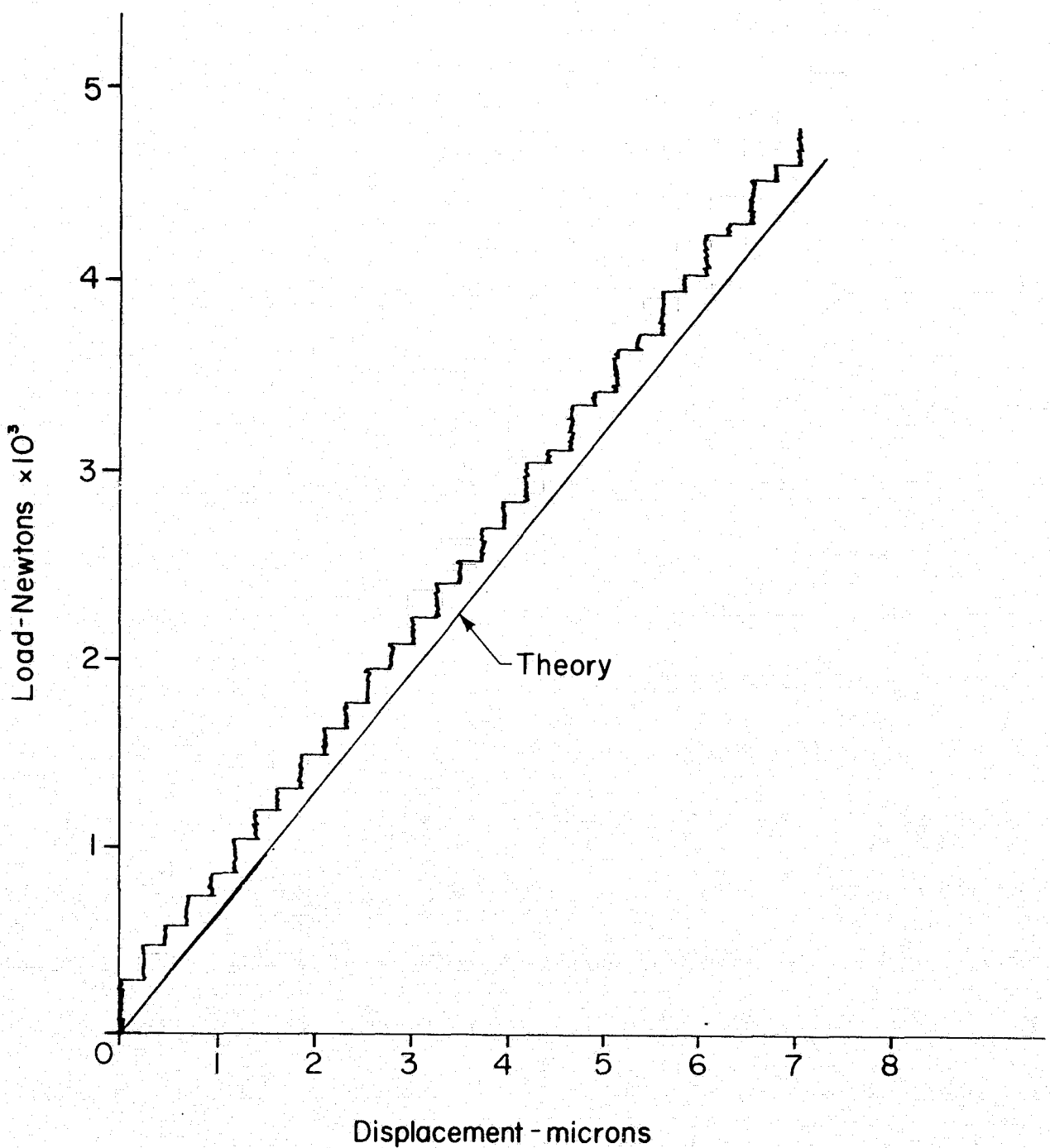

Figure 6.1 - Calibration results for displacement of center-cracked specimen.

"theory" line is computed from the formula on page 2.4 of reference [20], which is accurate to 0.6 percent. A value of 10.15×10^6 psi (70,000 MPa) was used in the calculation; this was obtained from an ASTM standard tension test. Figure 6.1 shows that the IDG can easily make useful measurements in this range.

6.3. Recommended Software Development

Both of the recommended improvements discussed in sections 4 and 5 would help measurement in this range. Extending the range of the small displacement technique would cover this range with a resolution of 0.004 microns. The resolution of the large displacement technique can easily be halved to 0.12 microns. If one wished to use the large displacement technique "as is," a plotting routine to plot points instead of steps would be useful.

7. DISPLACEMENTS ACROSS A FATIGUE CRACK

To demonstrate one application of this instrument, displacements as a function of applied load were measured on a tensile specimen with a large fatigue crack.

7.1. Specimen Description

The aluminum specimen was one that had been used for stress intensity factor measurements in reference [15]. It was 7075-651 aluminum, and the geometry of the fatigue crack in the central portion of the tensile specimen is shown in Figure 7.1. Indentations were applied as shown in that figure. These indentations were on the opposite side of the specimen from the side used by Macha et al. [15]. Details of the crack growth, etc., are given in reference [15].

7.2. IDG Measurements

All of the crack displacements were measured using the large displacement procedure. The range of the small displacement technique is not large enough at present.

Displacement across the fatigue crack at a position 7.12 mm from the crack tip as a function of load is shown in Figure 7.2. This plot is taken directly from the X-Y recorder, and when repeated runs were made, the displacement curves were identical. Also shown in Figure 7.2 are plots of the upper and lower figure motions (in terms of displacements). Both the

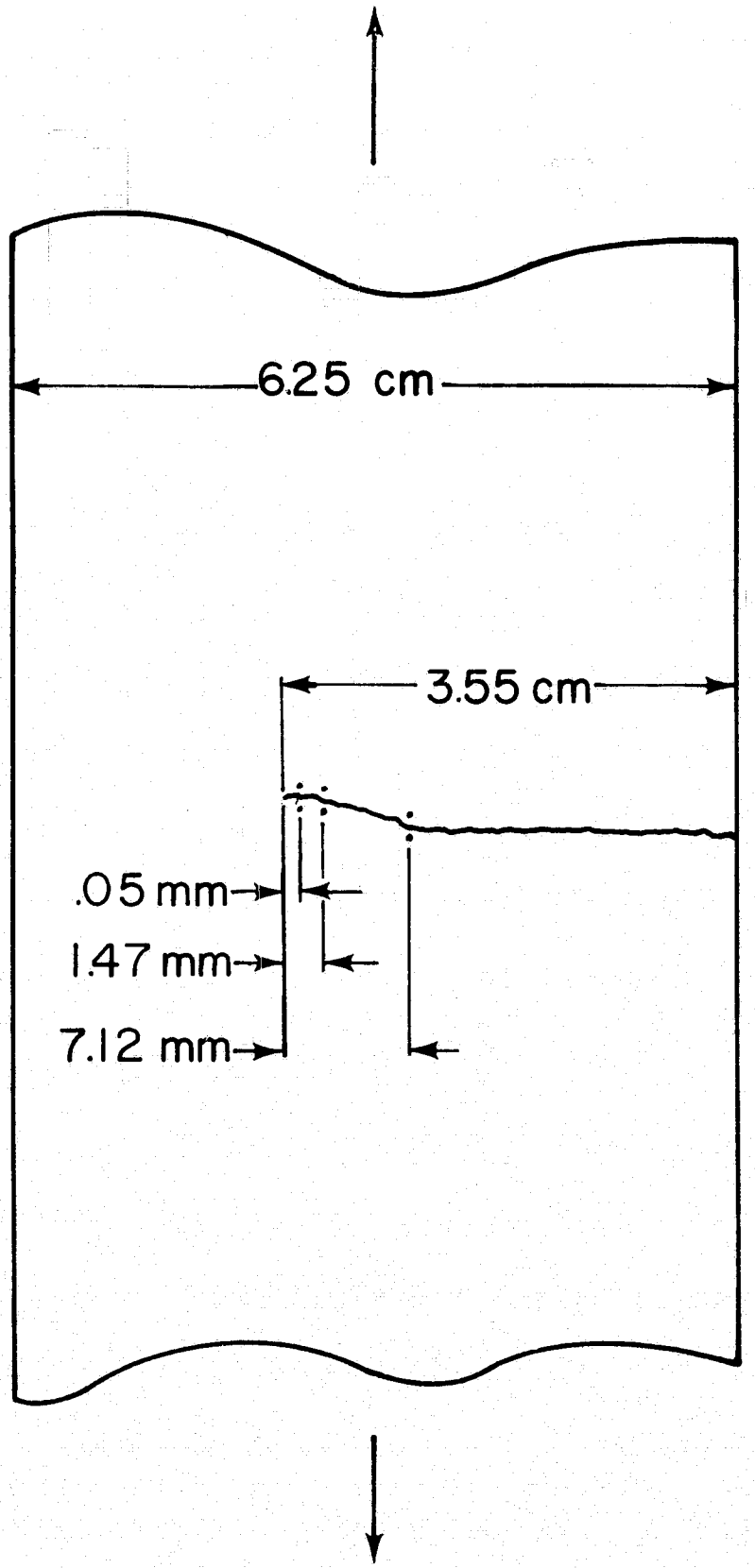

Figure 7.1 - Sketch of fatigue-cracked specimen.

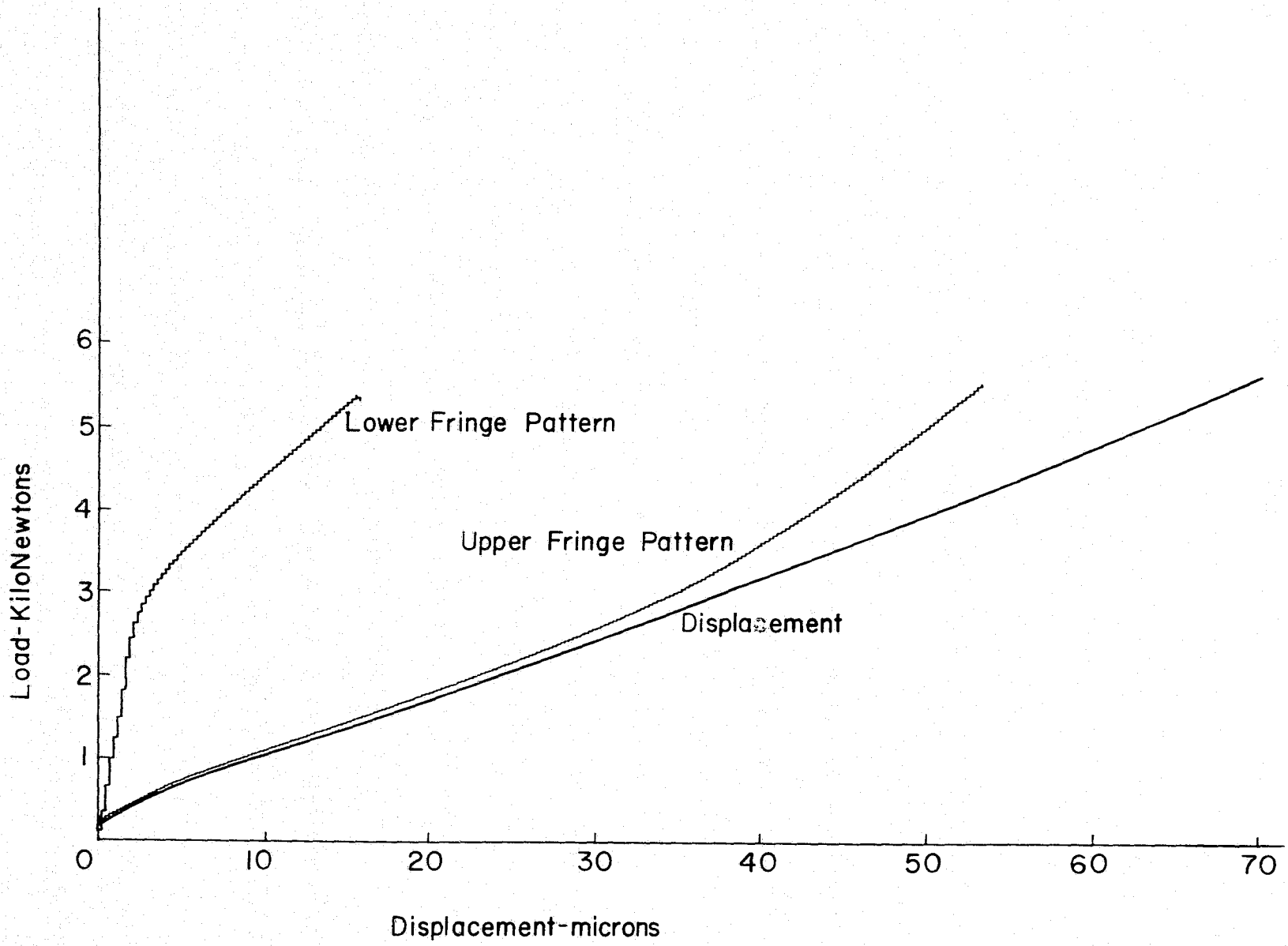

Figure 7.2 - Displacements across fatigue crack at a position 7.12mm from tip.

upper and lower fringes moved in a positive direction, so they add together parallel to the abscissa to produce the total displacement. It is interesting to note that the separate fringe motions are nonlinear with load, but add to produce a very linear load-displacement relation above a load of 2 KN. This nonlinearity of the separate motions is due to nonlinear rigid body motion in the testing machine; the rigid body motion is averaged out in the displacement curve. It is significant that the load separate fringe motions become linear at higher loads, indicating that the specimen and loading train are finally "straightened out." It appears that a more precisely aligned loading apparatus would be useful for these kinds of tests. The range of these measurements--about 70 microns--is dictated by the size of the laser beam and the amount of vertical rigid body motion of the indentations on the specimen.

Figure 7.3 presents the displacement curves and separate fringe motions for the indentations located 1.47 mm from the crack tip. The lower fringe pattern started out moving in a negative direction and then reversed to move toward the incident beam. This was observed visually, but could be interpreted from the region of large increase in load with no fringe increment (where the fringes were reversing direction). This means that the displacement curve is in error the two increments of negative motion, i.e., the displacement curve should be shifted two increments (0.48 microns) to the left. A software program that accounted for fringe direction would of course eliminate that error.

One of the tests run by Macha et al. [15] on this specimen was a load-displacement test with indentations at 1.32 mm from the crack tip. They used the slope of the linear portion of the curve to compute the stress intensity factor. Their measured slope was 212 newtons/micron. The slope of the load-displacement curve obtained at 1.47 mm on the opposite side of the same specimen is (from Figure 7.3) 215 newtons/micron. Such excellent agreement is almost certainly fortuitous, but the fact that two separate measurements on the same specimens using different versions of IDG data reduction in two separate laboratories is comforting.

One aspect of the comparison with the Macha et al. [15] experiments is extremely interesting. They measured the load-displacement relation soon (on the order of days) after the fatigue crack was grown, and their curve shows a large amount of closure, as indicated by the large load level at which the plot becomes linear (see Figure 7.4). In contrast, the

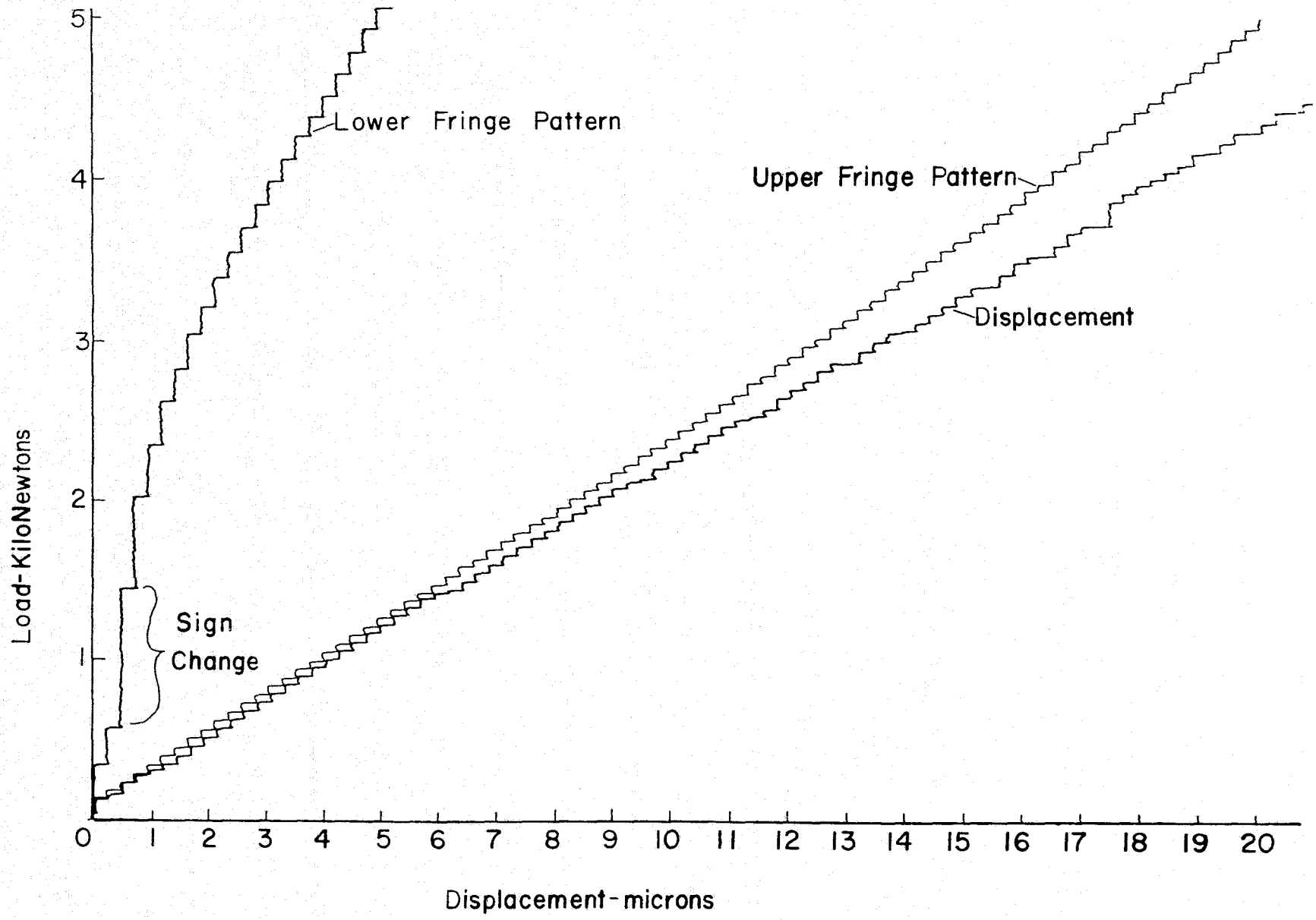

Figure 7.3 - Displacements across fatigue crack at a position 1.47mm from tip.

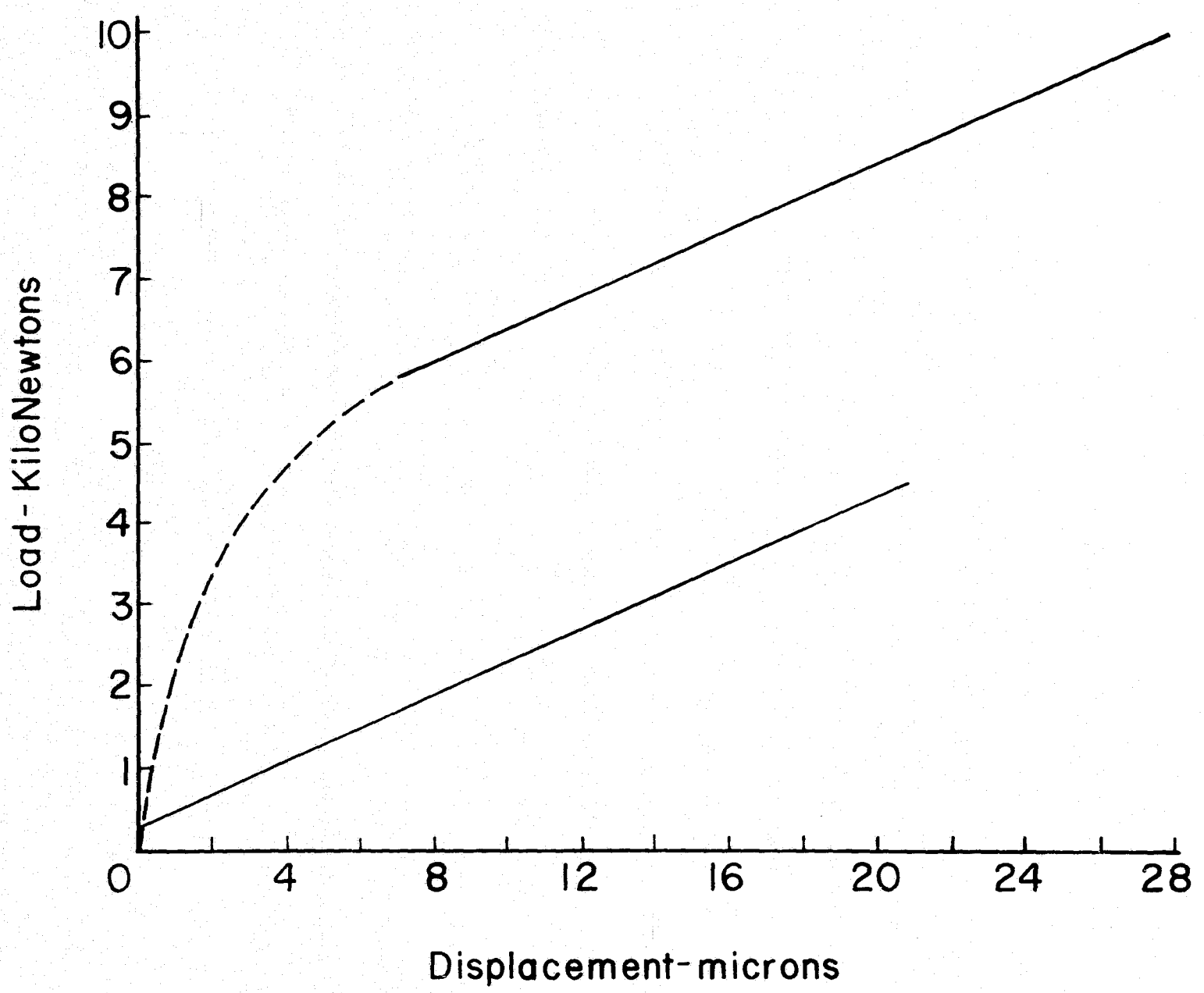

Figure 7.4 - Comparison of displacements at 1.47mm with earlier measurement on same specimen at 1.32mm by Macha et al (15).

current measurements--18 months later--show very little closure. It appears that a significant relaxation of the residual stresses around the crack tip occurred in this time.

Load-displacement at a location 0.05 mm from the crack tip is shown in Figure 7.5. Here the lower fringe pattern moves entirely in the negative direction, i.e., the fringe motion due to rigid body translation is larger than that due to relative displacement. This sign change was accounted for in the program, so there is no error in Figure 7.5. Note that the displacement curve lies between the fringe motion curves, in contrast to earlier figures. Note also that when a negative increment is added to the counter the displacement decreases; the curve is no longer of a "stair-step" nature. The plot here doesn't have a long linear region, though it tends to become linear at larger loads.

Figure 7.6 is a photomicrograph of the indentation located at 0.05 mm from the original crack tip and shows two mistakes in experimental procedure. First, the indentations should be symmetric about the crack; they are misplaced slightly and are 60 microns apart. The indentations are aligned parallel to the load axis of the specimen as intended, but the crack is slightly curved. The large dark region in the right side of Figure 7.6 is a crack grown by static overload--a second error. The load-displacement curve of Figure 7.5 was obtained after this overload, so it cannot be compared with earlier measurements.

8. DISCUSSION

It may be useful to compare the IDG with the other methods of measuring crack opening displacement in the neighborhood of crack tips and also to discuss some potential applications of the technique. Conclusions about the instrument development described in this report close this section.

8.1. Comparison with Other Techniques

The techniques for measuring surface crack opening displacement on opaque specimens are referenced in section 1 of this report. They include the foil gage bonded on its ends, the small clip gage, photomicrography, and the moiré technique.

In terms of the size of the transducer, the IDG is smaller than all but photomicrography. Reference [3] used a gage length of 76 microns, which is roughly the same as the 50-300 micron gage length of the IDG.

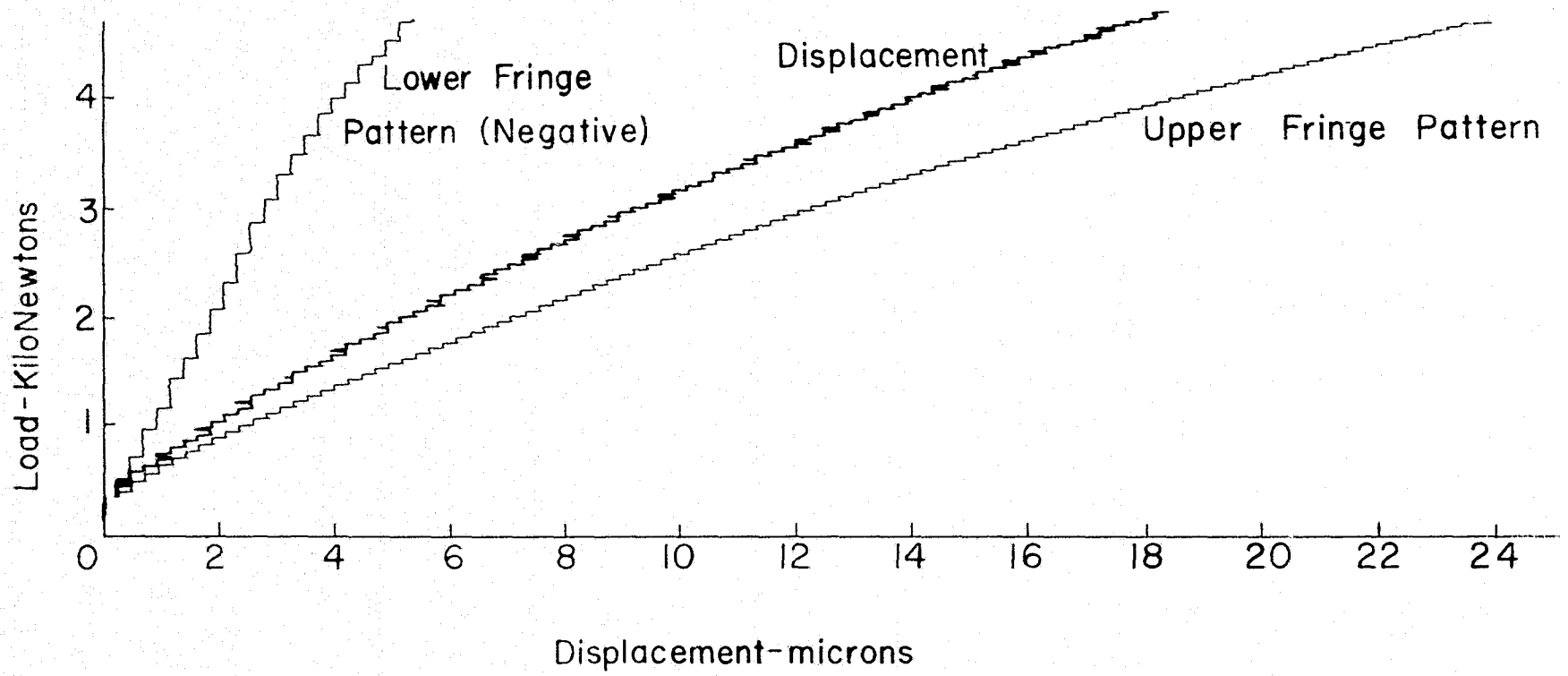

Figure 7.5 – Displacements across fatigue crack tip at a position 0.05mm from tip.

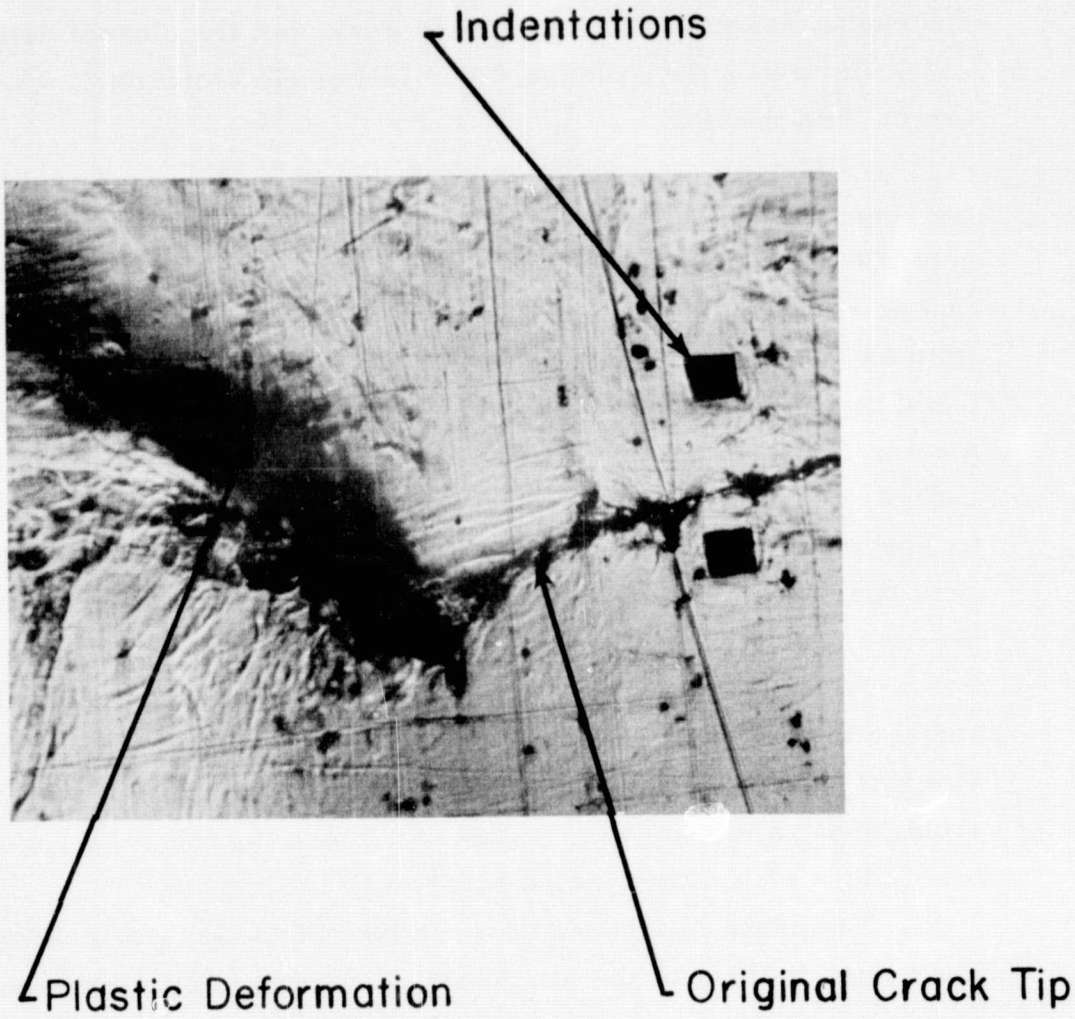

Figure 7.6 - Photomicrograph of indentations 0.05mm from tip. Indentations are 60 microns apart. The crack was extended "statically" by an accidental overload; the plastically deformed region is quite evident.

The small clip gage [1, 2] has a gage length of 1270 microns, and a typical foil gage installation for crack displacement measurement has a gage length of 2000 microns plus a gage width of the same order. The moiré technique applications [11] usually put their results in terms of strain, but the original fringes are related to displacement. The "size" of the moiré gage is difficult to evaluate from published work, but the closest data points to the crack tip are on the order of 0.030 inches (760 microns), which makes it larger than the IDG.

The scan rate of the current IDG is ~ 2400 scans per second in the large displacement configuration, which means that, if one would accept 100 points per cycle in fatigue testing (50 up and 50 down), one could test at a rate of 24 Hz. The clip gage is limited in frequency response by its mass and is usually used at 1 Hz or less. Supposedly the foil gage could be used at higher rates; it certainly is for dynamics strain measurements. However, no one has examined the foil gage used as a displacement gage at high frequency. Photomicrography and moiré are not real-time techniques, although motion pictures could be taken. One aspect of real-time operation needs to be emphasized: it permits the use of the crack displacement as a control in cyclic testing.

The IDG is not very difficult to use. Preparation of the specimen surface is straightforward and the application of the indentations is easy. The IDG would take about as much time for specimen preparation and data acquisition as the foil gage technique, more than the clip gage, and considerably less than either moiré or photomicrography.

The main difference between the IDG and other techniques that one has to worry about is the alignment of the specimen. Extraneous rigid body motions perpendicular to the specimen surface can lead to errors. This comment is included as a word of caution; the present and previous works show that it is not a serious problem.

8.2. Potential Applications of the IDG

While the computerized IDG as described in this report has some obvious advantages, the requirement of a complete minicomputer system is a drawback. Certainly the use of a minicomputer for the large displacement measurements is an "overkill." Work is currently underway to develop an analog counting circuit using photodiodes for detectors to produce a simpler IDG instrument based on the large displacement technique.

By virtue of its noncontacting nature, the IDG is potentially useful at high temperatures. Work of a preliminary nature [21] has been done to extend the technique to 2500°F in air. Pt-10% Rh tabs resist oxidation at such high temperatures, and an argon laser supplies sufficient power (~200 mw) at a short wavelength to maintain fringe visibility. There certainly seems to be no fundamental difficulty in extending the technique to high temperatures, but just how high is uncertain.

Creep measurements place strong restrictions on instrumentation because of the stability requirements of the transducer and electronics. The IDG is essentially a geometrical device, so the stability requirements are placed on the fixtures holding the detectors, specimen, etc. For this reason, it is likely that it would prove useful for creep--particularly high temperature creep--measurements.

8.3. Closing Comments

This computerized interferometric displacement gage has been demonstrated to be accurate on calibration specimens in a laboratory environment. Coupled with the attendant advantages of the IDG, i.e., small size and noncontacting, these verification tests show that the technique is potentially useful for a variety of displacement measurements. Displacement across a crack is easily measured with the IDG, but there are other areas, e.g., strain near stress concentrations, where it would be useful.

The fringe motion transducers based on oscillating mirrors and photomultiplier tubes has proven to be quite satisfactory. Electrical signals analog to the position of the fringes in space are produced with a high signal-to-noise ratio. Once these are fed into a minicomputer system, reasonably elementary programming converts the fringe motions into a displacement. More software development is needed to increase the range of the small displacement technique and account for direction with the large displacement technique. Given those developments, one would have a displacement measuring instrument with excellent resolution and range.

In summary, this first version of the computerized IDG is very promising. Further developments of software are likely to be quite productive in expanding the capabilities of the instrument.

9. REFERENCES

1. Elber, W., "The significance of fatigue crack closure," Damage Tolerance in Aircraft Structures, American Society for Testing and Materials, ASTM STP 486, 1971, pp. 230-242.

2. Elber, W., "Fatigue crack closure under cyclic tension," Engineering Fracture Mechanics 2, 1970, pp. 37-45.

3. Adams, N. J., "Fatigue crack closure at positive stresses," Engineering Fracture Mechanics 4, 1972, pp. 543-554.

4. Roberts, R., and R. A. Schmidt, "Observations of crack closure," International Journal of Fracture Mechanics 8, 1972, pp. 469-471.

5. Buck, O., C. L. Ho, H. L. Marcus, and R. B. Thompson, "Rayleigh waves for continuous monitoring of a propagating crack front," Stress Analysis and Growth of Cracks, Proceedings of the 1971 National Symposium on Fracture Mechanics, Part I, ASTM 513, 1972, pp. 280-291.

6. Shih, T. T., and R. P. Wei, "A study of crack closure in fatigue," Engineering Fracture Mechanics 6, 1974, pp. 19-32.

7. Smith, C. W., "Use of three-dimensional photoelasticity and progress in related areas," Experimental Techniques in Fracture Mechanics 2, Society for Experimental Stress Analysis, 1975, pp. 3-58.

8. Dudderar, T. D., and H. J. Gorman, "The determination of Mode I stress-intensity factors by holographic interferometry," Experimental Mechanics 13, April 1973, pp. 145-149.

9. Sommer, E., "An optical method for determining the crack-tip stress intensity factor," Engineering Fracture Mechanics 1, 1970, pp. 705-718.

10. Crosley, P. B., S. Mostovoy, and E. J. Ripling, "An optical-interference method for experimental stress analysis of cracked structures," Engineering Fracture Mechanics 3, 1971, pp. 421-433.

11. Liu, H. W., and J. S. Ke, "Moiré method," Experimental Techniques in Fracture Mechanics 2, Society for Experimental Stress Analysis, 1975, pp. 111-165.

12. Packman, P. F., "The role of interferometry in fracture studies," Experimental Techniques in Fracture Mechanics 2, Society for Experimental Stress Analysis, 1975, pp. 59-87.

13. Sharpe, W. N., Jr., and A. F. Grandt, Jr., "A laser interferometric technique for crack surface displacement measurements," Proceedings of the 20th International Instrumentation Symposium of the Instrument Society of America, Albuquerque, New Mexico, May 1974.

14. Sharpe, W. N., Jr., D. M. Corbly, and A. F. Grandt, Jr., "Effects of rest time on fatigue crack retardation and observations of crack closure," Fatigue Crack Growth under Spectrum Loads, ASTM STP 595, American Society for Testing and Materials, 1976, pp. 61-77.

15. Macha, D. M., W. N. Sharpe, Jr., and A. F. Grandt, Jr., "A laser interferometry method for experimental stress intensity factor calibration," presented at Ninth National Symposium on Fracture Mechanics, Pittsburgh, Pennsylvania, August 1975.

16. Sharpe, W. N., Jr., "Interferometric surface strain measurement," International Journal of Nondestructive Testing 3, 1971, pp. 56-76.

17. Sharpe, W. N., Jr., "The interferometric strain gage," Experimental Mechanics 8, April 1968, pp. 164-170.

18. Sharpe, W. N., Jr., "Dynamic plastic response of foil gages," Experimental Mechanics 10, October 1970, pp. 408-415.

19. Sharpe, W. N., Jr., "A short gage-length optical gage for small strain," Experimental Mechanics 14, 1974, pp. 373-377.

20. Tada, H., P. C. Paris, and G. R. Irwin, The Stress Analysis of Cracks Handbook, Del Research Corporation, Hellertown, Pennsylvania, 1973.

21. Sharpe, W. N., Jr., "Preliminary development of an interferometric strain gage for use on nosetip materials subjected to thermal shock," draft of final technical report on Air Force Contract F 33615-75-C-5230, June 1976.

ADDENDUM

This addition to the original report describes further software developments for the large-displacement technique. These were prepared by Mr. Dennis Anderson, a computer science major, during the summer of 1976--after the original grant had expired. Since this represents a great improvement over the first version of the large-displacement program, it is desirable to include it.

The second version is different from the one described in Section 5 in that it:

1) senses the sign of each fringe motion and accounts for it in the computation of displacement,
2) measures cyclic displacement,
3) has a resolution of 0.12 micron.

The second version incorporates all the recommendations of Section 5.5. The new program is described and then typical results are presented. These typical results are in addition to those presented in Sections 6 and 7 of the original report.

LARGE DISPLACEMENT MEASUREMENT--
Second Version of Software

The program utilizes the scanning mirrors to sample each fringe pattern at three separate positions for each scan. This scan is adjusted so that the angular rotation between positions 1 and 3 is less than one-half of one fringe spacing apart. These three voltages (V_1, V_2, V_3) go into two counting routines: A comparing $V_2 - V_1$, and B comparing $V_3 - V_2$. The two counting routines are similar to the one described in Figure 5.1, i. e., they determine whether a maximum or minimum has passed and feed this information into a total increment counter.

Direction of motion of each fringe pattern must be established at the beginning of the test. Counter A and counter B must <u>each</u> sense a maximum or minimum before the direction can be established. The order in which these occur is important and Table A-1 shows the eight possible sequences. Table A-1 defines eight possible states, each state consisting of not only a maximum or minimum in counter A or B, but of the order in which they occurred. As soon as the separate counters are activated, the appropriate increment (+ or -) is fed to the total increment counter. As the fringes continue to move, either counter A or B will be activated. The order in which this happens, referenced to the previous state, determines whether the increment is + or -. Table A-2 shows the possible subsequent <u>individual</u> events for each state and the sign of the increment as well as the new state. Note that some individual events are prohibited; e. g., if in state 0, a maximum on counter A cannot be the next event. Furthermore, if, as in state 0, the last event was a maximum on B ($V_3 - V_2 > 0$) and the fringe reverses direction, the next event will appear to be a minimum on B ($V_3 - V_2 < 0$).

The rotation of the mirrors determines the spacing along the fringe of the input voltages V_1, V_2, and V_3. This is controlled by a D/A output to the moveable mirror. The voltage to be output can be set as a decimal number (0-4095) corresponding to (0-10) volts. Again, this total separation must be less that 1/2 fringe spacing.

The voltage increment is a decimal number which defines the absolute difference between input voltages which must be exceeded before a significant change is considered to exist. This value too can be set easily prior to program execution and is used to compensate for electrical noise of the system.

Motion	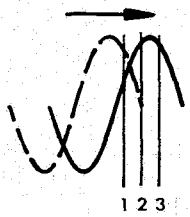	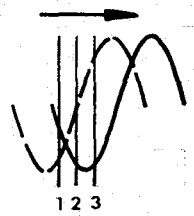	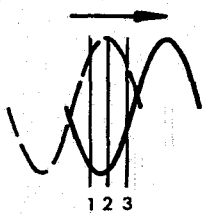	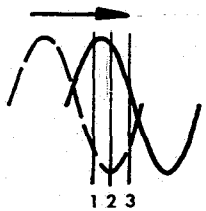
Sequence	Max A, Max B	Min A, Min B	Max B, Min A	Min B, Max A
State	0	1	2	3

Motion	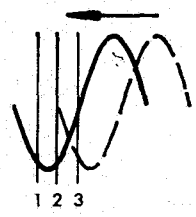	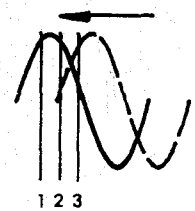	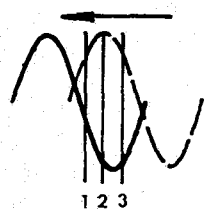	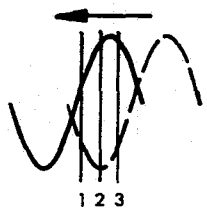
Sequence	Min B, Min A	Max B, Max A	Max A, Min B	Min A, Max B
State	4	5	6	7

Table A1 - Schematic of various fringe motion sequences. The dashed fringe is the position before motion; the solid fringe the position after a max or min has been observed on counter A or B. The designated state is stored in the minicomputer and used to give the proper sign to subsequent motion.

Existing State	Next Input Detected			
	Max A	Min A	Max B	Min B
0	x	+,2	x	-,6
1	+,3	x	-,7	x
2	-,5	x	x	+,1
3	x	-,4	+,0	x
4	+,3	x	-,7	x
5	x	+,2	x	-,6
6	x	-,4	+,0	x
7	-,5	x	x	+,1

Table A2. The entries in the table list the sign of the increment output to the totalizing counter and the next state of fringe motion. For example, if a fringe is in state 0 and sees a minimum on counter A, it will output a + increment and change the state to 2.

The output counter for this program increments or decrements for both counter A and counter B every time a maximum or minimum is recorded by either channel 1 or 2. Thus for a single channel there exists four counts for each single fringe shift. Since there are two channels, the resolution of the system is $1/8^{th}$ of a fringe shift or approximately 0.12 micron.

TYPICAL CYCLIC DISPLACEMENTS

Displacements of the center-cracked specimen used in Section 6 were recorded with the new version. Figure A-1 shows the displacement from each fringe pattern as well as the total displacement. Note that each fringe pattern "sees" essentially the same displacement. This is because the specimen is so compliant that the relative displacement across the slot is much larger than any rigid body motion of the slot. Note also the finer resolution compared to Figure 6.1.

Figure A-2 shows the displacement of the center-cracked specimen subjected to four cycles of loading/unloading. The repeatability and lack of hysteresis is excellent.

The edge-cracked specimen of Figure 7.1 was used for cyclic measurements; new indentations were located 0.32 mm from the tip of the crack. Figures A-3 and A-5 show the individual fringe pattern motion and the resulting displacement. The indentations close to the fatigue crack tip separate a smaller amount relative to the rigid-body motion, so the lower fringe pattern goes negative. Comparing Figure A-3 with Figures 7.3 and 7.5 shows the improvement with the new program; the sign of each fringe pattern is automatically accounted for.

Figures A-4 and A-6 show cyclic loadings for the edge-cracked specimen. The repeatability is excellent; however, the gage closest to the crack tip shows some hysteresis on unloading.

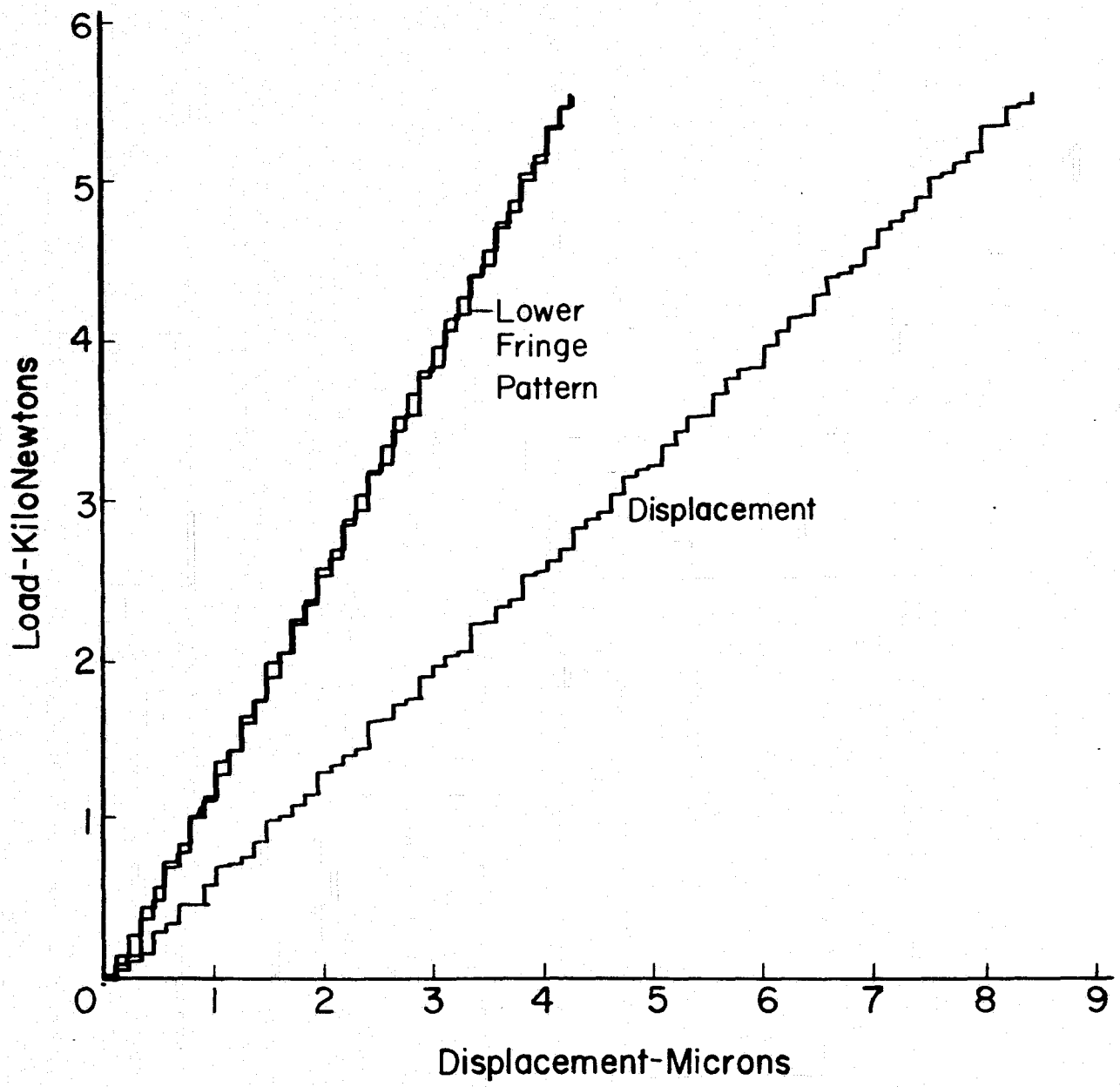

Figure A1. Displacements of a center-cracked specimen.

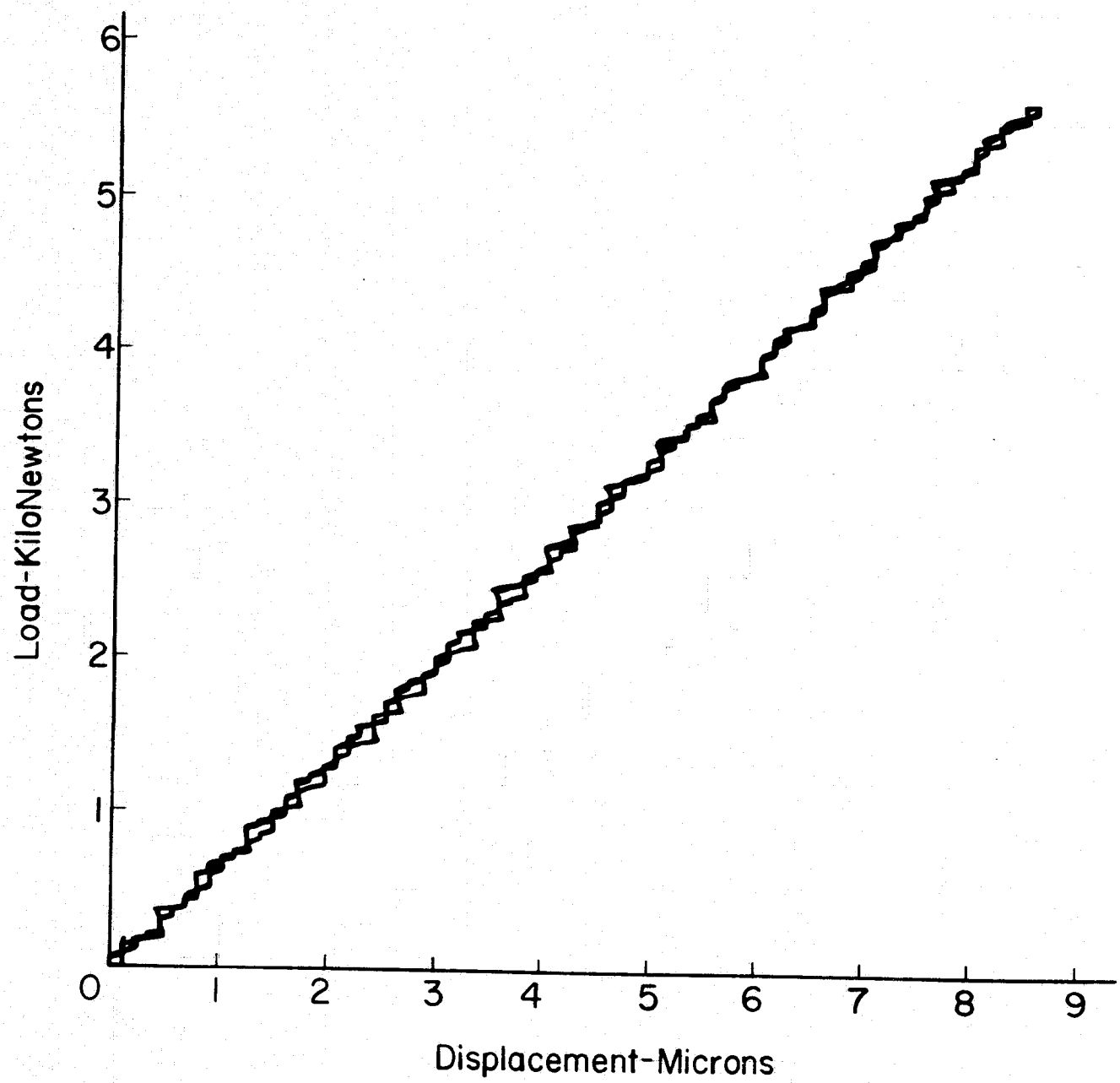

Figure A2. Cyclic displacements (4 cycles) of a center-cracked specimen.

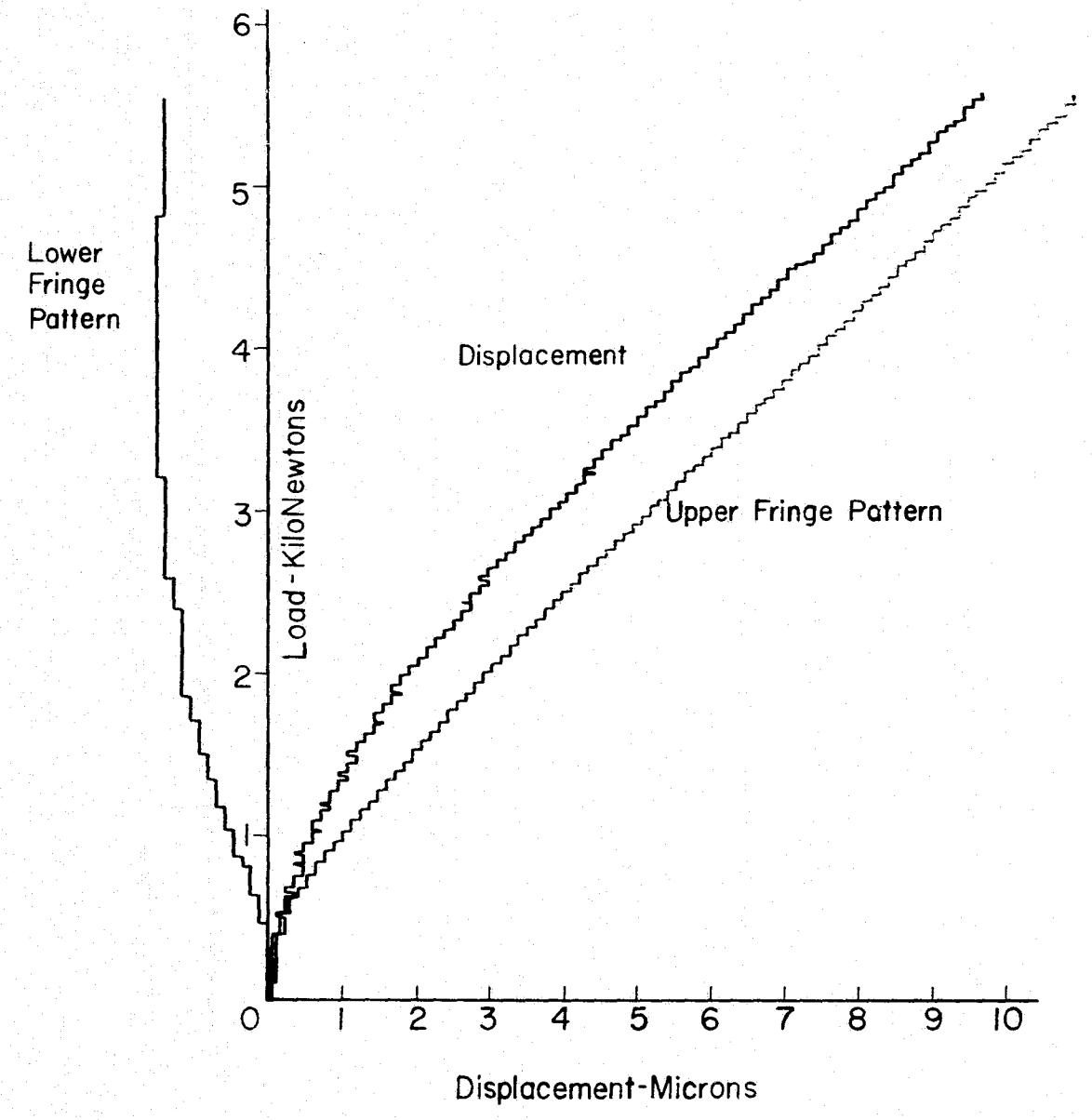

Figure A3. Displacements of an edge-cracked specimen at a position 0.32 mm from the crack tip.

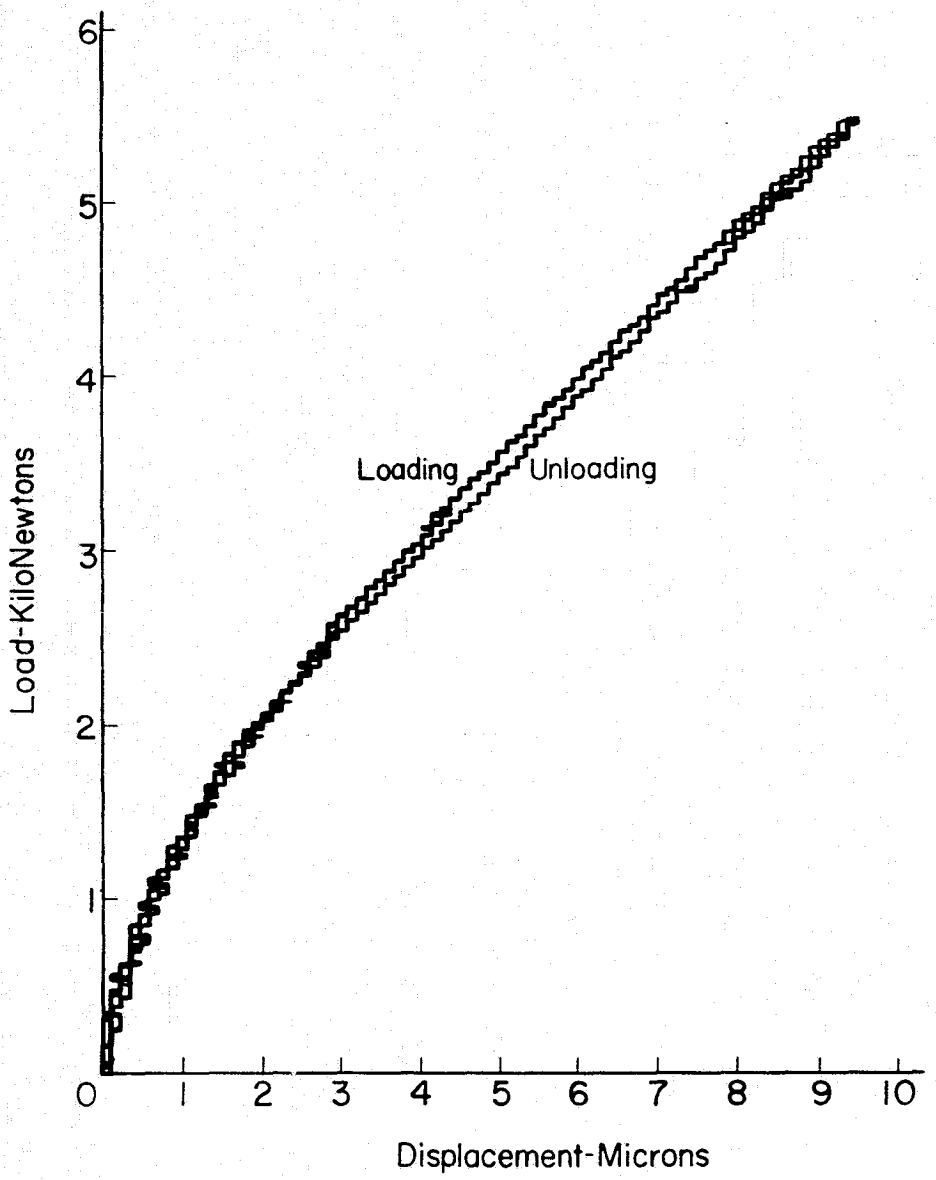

Figure A4. Cyclic displacements (4 cycles) of the specimen of Figure A3.

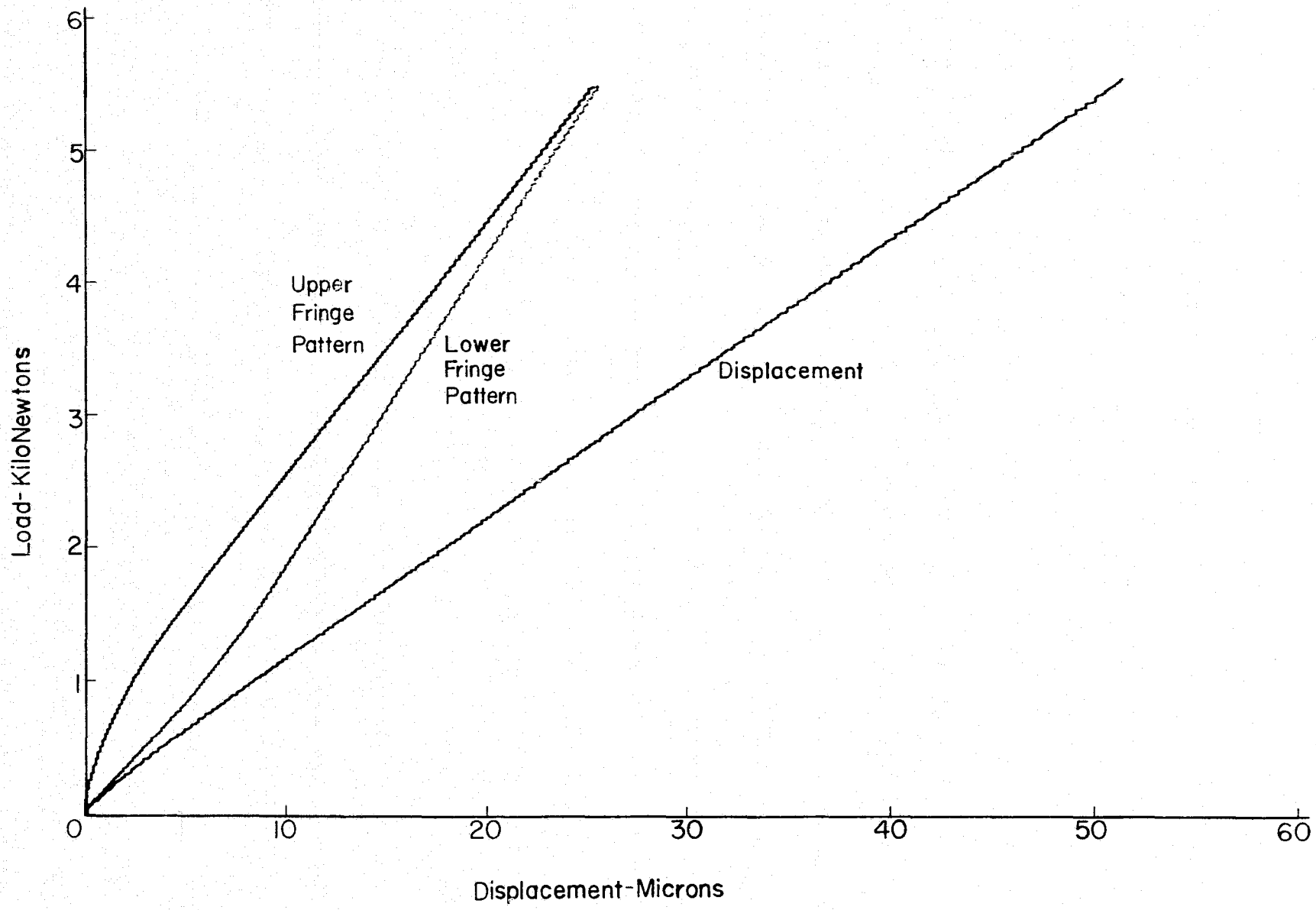

Figure A5. Displacements of an edge-cracked specimen at a position 5.01 mm from the crack tip.

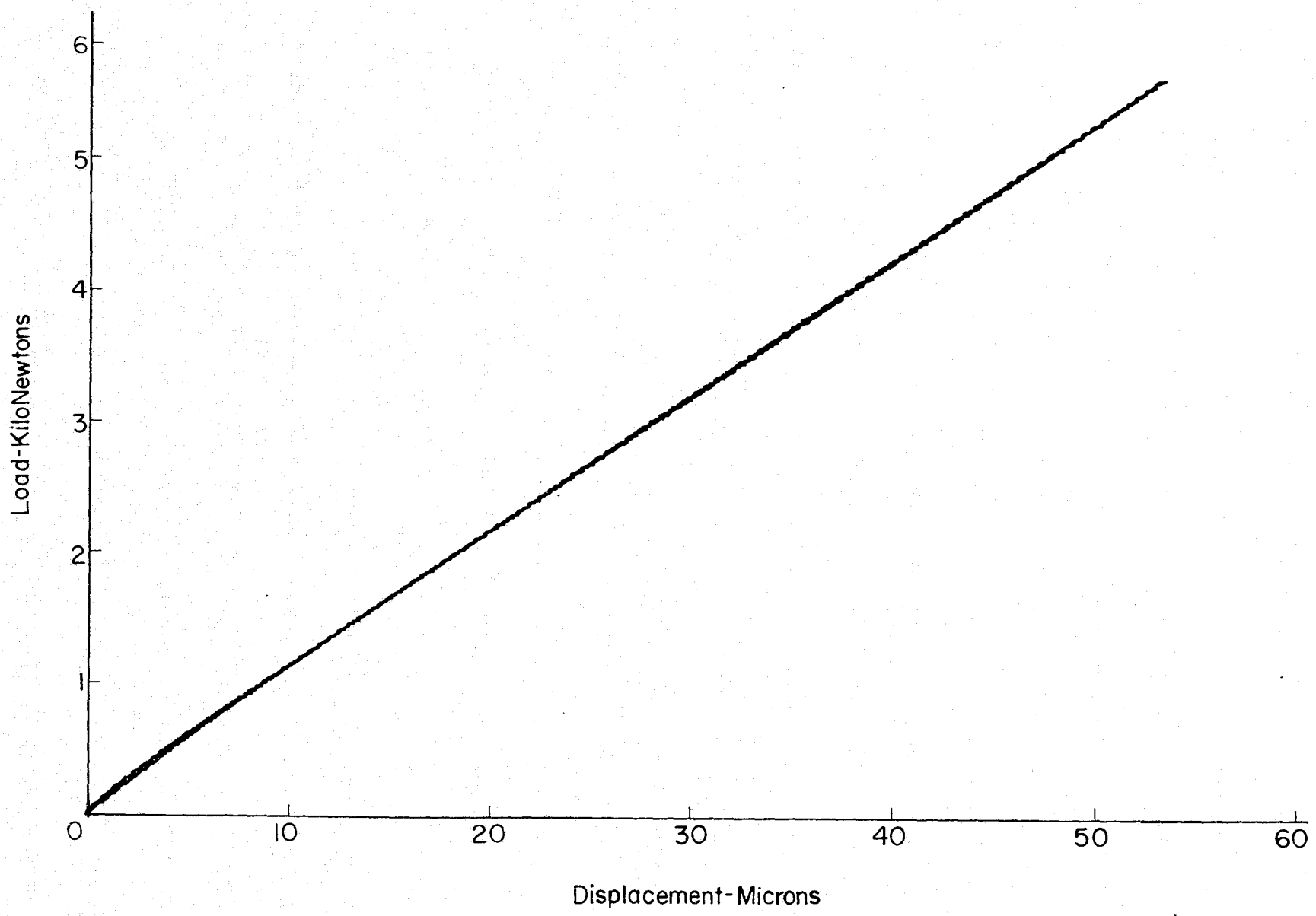

Figure A6. Cyclic displacements (4 cycles) of the specimen of Figure A5.